MATERIALS AND METHODS

Human cell lines

Human skin fibroblasts and keratinocytes were obtained from skin biopsies. Fibroblasts were grown in Dulbecco's modified Eagle's medium (DMEM) containing 10% fetal calf serum, and keratinocytes were cultured in H. Green keratinocyte-specific medium (Green *et al.*, 1979). Keratinocytes and fibroblasts were kindly provided by Professor Ben-Basst Laboratory, Hadassah University Hospital, Jerusalem, Israel. Cells were passaged weekly by trypsinization. Bone marrow endothelial cells are microvascular endothelial cells isolated from human bone marrow aspirates. The bone marrow endothelial cell-1 cell line was kindly provided by S Rafii. This cell line was generated by introducing the SV40-large T antigen into an early passage of primary bone marrow endothelial cell, and it has retained the morphology, phenotype, and function of the primary bone marrow endothelial cell. The bone marrow endothelial cell-1 cells were cultured in a complete DMEM and were passaged weekly by trypsinization.

Immunohistochemistry and *in vitro* scratched assay

Skin tissue samples were routinely fixed with formalin and embedded in paraffin. Antigen retrieval was performed in ethylenediaminetetraacetic acid buffer for 15 minutes in microwave, and sections were stained with mAB (MAB 350) (R&D Systems Inc., Minneapolis, MN) for CXCL12 (1:100) mAB' against cytokeratins 1, 5, 15, and 10 (M0630) (DAKO, Glostrup, Denmark) and mAB anti-vimentin (M7020) (DAKO), mAB against rat CXCR4 (Torrey Pines Biolabs, Houston, TX), using biotinylated secondary polymer (87–9,963) (Zymed) based on standard indirect avidin-biotin horseradish peroxidase method, according to the manufacturer's instructions. 3-amino-9-ethylcarbazole was used for color development and sections were counterstained with hematoxylin. Cell immunohistochemistry staining: keratinocyte and fibroblast monolayers were grown in a tissue culture 6 mm plates. Then, cells were scratched using a 200 μl pipette, washed three times with phosphate - buffered saline (PBS), and grown in DMEM with 1% fetal calf serum. After 2 days, cells were fixed using 4% paraformaldehyde and stained for the chemokine CXCL12 as described previously.

ELISA assay and RT-PCR

ELISA assays for CXCL12 and IL-8 in burn fluids of fibroblast and keratinocyte medium were performed using the Quantikine kit (R&D Systems Inc., Minneapolis, Minnesota), according to the manufacturer's instructions. The expression levels of the chemokine CXCL12 and the chemokine receptor CXCR4 were determined by RT-PCR analysis. Total RNA was isolated from primary fibroblast and keratinocyte cultures. Each RNA sample was subjected to cDNA synthesis, and then semiquantative PCR was performed with specific primers at appropriate annealing temperatures. The resulting PCR products were separated on 1% agarose gel.

Transwell migration assays

Rat peripheral blood cells were loaded on Ficoll (Histopaque-1077-1, Sigma), and the peripheral blood mononuclear cells were isolated. Rat peripheral blood mononuclear cell migration was assessed in 24-well chemotaxis chambers (6.5-mm diameter, 5-mm pore polycarbonate transwell culture insert; Costar, Cambridge, Massachusetts). RPMI 1640 (600 μl) with 1% BSA (migration buffer) with or without 100 ng/ml of CXCL12α (Peprotech, Rehovot, Israel) were added to the lower wells, and 2×10^5 cells suspended in 100 μl of RPMI 1640 with 1% BSA were added to the upper wells. After 3 hours incubation, the membrane was removed and migrating cells were counted for 1 minute using fluorescence activated cell sorter.

Tissue collection, histological evaluation of the burn lesion

Human skin tissue samples were obtained from the Plastic Surgery Department, Souraski Medical Center, Tel-Aviv. In order to examine the different phases in burn wound healing and the involvement of the chemokine CXCL12 and the receptor CXCR4, the following experiments were carried out. Wistar female rats were anesthetized and their back was shaved. Burns (1 cm^2) were inflicted with a metal rod that has been immersed in a hot boiling water bath and laid on the posterior part of the hip and back for 2–3 seconds. All experiments were approved by the Animal care committee of the Medical Center, Tel-Aviv and the Hebrew University. All the material collected from human specimens was approved by Tel-Aviv Sourasky Medical Center Institutional Committee and in adherence to the Declaration of Helsinki Principles. Heterozygous mice bearing a GFP reporter knocked-in allele to the CX3CR1 locus (Qu *et al.*, 2004) were maintained at the Weizmann Institute of Science Animal Facility. Each group of three rats was injected subcutaneously with either PBS, anti-CXCR4, or with 4F-benzoyl-TN14003 to the burned area. Animals were killed at the indicated times after burn infliction: 0, 6 hours, 1 day, 3 days, 5 days, and 7 days. Histopathological diagnosis was confirmed for each specimen. Histological sections were prepared from formalin-fixed, paraffin-embedded tissues stained with hematoxylin and eosin. The evaluation to the level of epithelialization and white blood cells in the epidermis and dermis was made to each section by a scale from 1 to 5. The sections were scored by two independent pathologists. Treated rats were injected subcutaneously to the burned area with one of the following: PBS, mAB against rat CXCR4, the small peptide CXCR4 inhibitor, or 4F-benzoyl-TN14003. All animals were killed 120 hours after injury. Histopathological diagnosis was confirmed for each specimen. Histological sections were prepared from formalin-fixed, paraffin-embedded tissues stained with hematoxylin and eosin. The evaluation to the level of epithelialization and white blood cells in the dermis was made to each section by a scale from 1 to 5. The grading scale was as follows: 0 = no inflammation or epithelialization; 1 = low inflammation or epithelialization; 2 = low to moderate inflammation or epithelialization; 3 = moderate inflammation or epithelialization; 4 = high inflammation or epithelialization; and 5 = very high inflammation or epithelialization.

Swine burned skin paraffin-embedded sections were provided by the Laboratory of Experimental Surgery, Hadassah University Hospital, Jerusalem, Israel. All experiments were approved by the Animal Care Committee of the Hebrew University. Burn blister fluid collection was collected at the Plastic Surgery Department, Souraski Medical Center, Tel-Aviv, Israel as a medical procedure. The blister fluid was examined for the chemokine CXCL12 levels by ELISA assay, and for the levels of IL-8.

Statistical analysis

Results are expressed as mean $\pm$ SD. Statistical differences were determined by an analysis of two-tailed Student's *t*-test.

CONFLICT OF INTEREST

The authors state no conflict of interest.

ACKNOWLEDGMENTS

We thank Mery Clausen (Gene Therapy Institute, Hadassah Hospital) for technical assistance. This study was supported by the Horwitz Foundation, the Israeli Ministry of Science – the Knowledge Center for Gene Therapy, the Blum Foundation, and the Grinspoon Foundation.

REFERENCES

Aiuti A, Webb IJ, Bleul C, Springer T, Gutierrez-Ramos JC (1997) The chemokine SDF-1 is a chemoattractant for human CD34+ hematopoietic progenitor cells and provides a new mechanism to explain the mobilization of CD34+ progenitors to peripheral blood. *J Exp Med* 185:111–20

Askari AT, Unzek S, Popovic ZB, Goldman CK, Forudi F, Kiedrowski M *et al.* (2003) Effect of stromal-cell-derived factor 1 on stem-cell homing and tissue regeneration in ischaemic cardiomyopathy. *Lancet* 362:697–703

Ceradini DJ, Kulkarni AR, Callaghan MJ, Tepper OM, Bastidas N, Kleinman ME *et al.* (2004) Progenitor cell trafficking is regulated by hypoxic gradients through HIF-1 induction of SDF-1. *Nat Med* 10:858–64

Clark RA (1988) *The molecular and cellular biology of wound repair*, 2nd ed. New York: Kluwer Academic Plenum Publishers

Cotran RS, Kumar V, Collins T (1999) *Pathologic basis of disease*, 6th ed. Philadelphia: W.B. Saunders Company

Doitsidou M, Reichman-Fried M, Stebler J, Koprunner M, Dorries J, Meyer D *et al.* (2002) Guidance of primordial germ cell migration by the chemokine SDF-1. *Cell* 111:647–59

Faunce DE, Llanas JN, Patel PJ, Gregory MS, Duffner LA, Kovacs EJ (1999) Neutrophil chemokine production in the skin following scald injury. *Burns* 25:403–10

Gibran NS, Ferguson M, Heimbach DM, Isik FF (1997) Monocyte chemoattractant protein-1 mRNA expression in the human burn wound. *J Surg Res* 70:1–6

Gillitzer R, Goebeler M (2001) Chemokines in cutaneous wound healing. *J Leukocyte Biol* 69:513–21

Gonzalo JA, Lloyd CM, Peled A, Delaney T, Coyle AJ, Gutierrez-Ramos JC (2000) Critical involvement of the chemotactic axis CXCR4/stromal cell-derived factor-1 α in the inflammatory component of allergic airway disease. *J Immunol* 165:499–508

Green H, Kehinde O, Thomas J (1979) Growth of cultured human epidermal cells into multiple epithelia suitable for grafting. *Proc Natl Acad Sci USA* 76:5665–8

Hitchon C, Wong K, Ma G, Reed J, Lyttle D, El-Gabalawy H (2002) Hypoxia-induced production of stromal cell-derived factor 1 (CXCL12) and vascular endothelial growth factor by synovial fibroblasts. *Arthritis Rheum* 46:2587–97

Iocono JA, Colleran KR, Remick DG, Gillespie BW, Ehrlich HP, Garner WL (2000) Interleukin-8 levels and activity in delayed-healing human thermal wounds. *Wound Repair Regen* 8:216–25

Lukacs NW, Berlin A, Schols D, Skerlj RT, Bridger GJ (2002) AMD3100, a CXCR4 antagonist, attenuates allergic lung inflammation and airway hyperreactivity. *Am J Pathol* 160:1353–60

Ma Q, Jones D, Borghesani PR, Segal RA, Nagasawa T, Kishimoto T *et al.* (1998) Impaired B-lymphopoiesis, myelopoiesis, and derailed cerebellar neuron migration in CXCR4- and SDF-1-deficient mice. *Proc Natl Acad Sci USA* 95:9448–53

McGrath KE, Koniski AD, Maltby KM, McGann JK, Palis J (1999) Embryonic expression and function of the chemokine SDF-1 and its receptor, CXCR4. *Dev Biol* 213:442–56

Nagasawa T, Hirota S, Tachibana K, Takakura N, Nishikawa S, Kitamura Y *et al.* (1996) Defects of B-cell lymphopoiesis and bone-marrow myelopoiesis in mice lacking the CXC chemokine PBSF/SDF-1. *Nature* 382:635–8

Nagase H, Kudo K, Izumi S, Ohta K, Kobayashi N, Yamaguchi M *et al.* (2001a) Chemokine receptor expression profile of eosinophils at inflamed tissue sites: decreased CCR3 and increased CXCR4 expression by lung eosinophils. *J Allergy Clin Immunol* 108:563–9

Nagase H, Miyamasu M, Yamaguchi M, Fujisawa T, Kawasaki H, Ohta K *et al.* (2001b) Regulation of chemokine receptor expression in eosinophils. *Int Arch Allergy Immunol* 125:1129–32

Nagase H, Miyamasu M, Yamaguchi M, Fujisawa T, Ohta K, Yamamoto K *et al.* (2000) Expression of CXCR4 in eosinophils: functional analyses and cytokine-mediated regulation. *J Immunol* 164:5935–43

Ono I, Gunji H, Zhang JZ, Maruyama K, Kaneko F (1995) A study of cytokines in burn blister fluid related to wound healing. *Burns* 21: 352–5

Pablos JL, Amara A, Bouloc A, Santiago B, Caruz A, Galindo M *et al.* (1999) Stromal-cell derived factor is expressed by dendritic cells and endothelium in human skin. *Am J Pathol* 155:1577–86

Peled A, Petit I, Kollet O, Magid M, Ponomaryov T, Byk T *et al.* (1999) Dependence of human stem cell engraftment and repopulation of NOD/SCID mice on CXCR4. *Science* 283:845–8

Petit I, Szyper-Kravitz M, Nagler A, Lahav M, Peled A, Hablea L *et al.* (2002) G-CSF induces stem cell mobilization by decreasing bone marrow SDF-1 and up-regulating CXCR4. *Nat Immunol* 3:687–94

Piccolo MT, Wang Y, Verbrugge S, Warner RL, Sannomiya P, Piccolo NS *et al.* (1999) Role of chemotactic factors in neutrophil activation after thermal injury in rats. *Inflammation* 23:371–85

Ponomaryov T, Peled A, Petit I, Taichman RS, Habler L, Sandbank J *et al.* (2000) Induction of the chemokine stromal-derived factor-1 following DNA damage improves human stem cell function. *J Clin Invest* 106:1331–9

Qu C, Edwards EW, Tacke F, Angeli V, Llodra J, Sanchez-Schmitz G *et al.* (2004) Role of CCR8 and other chemokine pathways in the migration of monocyte-derived dendritic cells to lymph nodes. *J Exp Med* 200: 1231–41

Schioppa T, Uranchimeg B, Saccani A, Biswas SK, Doni A, Rapisarda A *et al.* (2003) Regulation of the chemokine receptor CXCR4 by hypoxia. *J Exp Med* 198:1391–402

Singer AJ, Clark RA (1999) Cutaneous wound healing. *N Engl J Med* 341:738–46

Smith JM, Johanesen PA, Wendt MK, Binion DG, Dwinell MB (2005) CXCL12 activation of CXCR4 regulates mucosal host defense through stimulation of epithelial cell migration and promotion of intestinal barrier integrity. *Am J Physiol Gastrointest Liver Physiol* 288:316–26

Spies M, Dasu MR, Svrakic N, Nesic O, Barrow RE, Perez-Polo JR *et al.* (2002) Gene expression analysis in burn wounds of rats. *Am J Physiol Regul Integr Comp Physiol* 283:918–30

Struzyna J, Pojda Z, Braun B, Chomicka M, Sobiczewska E, Wrembel J (1995) Serum cytokine levels (IL-4, IL-6, IL-8, G-CSF, GM-CSF) in burned patients. *Burns* 21:437–40

Tamamura H, Hori A, Kanzaki N, Hiramatsu K, Mizumoto M, Nakashima H *et al.* (2003) T140 analogs as CXCR4 antagonists identified as anti-metastatic agents in the treatment of breast cancer. *FEBS Lett* 550:79–83

Wald O, Pappo O, Safadi R, Dagan-Berger M, Beider K, Wald H *et al.* (2004) Involvement of the CXCL12/CXCR4 pathway in the advanced liver disease that is associated with hepatitis C virus or hepatitis B virus. *Eur J Immunol* 34:1164–74

Yang J, Torio A, Donoff RB, Gallagher GT, Egan R, Weller PF *et al.* (1997) Depletion of eosinophil infiltration by anti-IL-5 monoclonal antibody (TRFK-5) accelerates open skin wound epithelial closure. *Am J Pathol* 51:1813–9

Zou YR, Kottmann AH, Kuroda M, Taniuchi I, Littman DR (1998) Function of the chemokine receptor CXCR4 in haematopoiesis and in cerebellar development. *Nature* 393:595–9

Available online at www.sciencedirect.com
SCIENCE DIRECT
Tetrahedron
ELSEVIER
Tetrahedron 62 (2006) 1416–1424

Application of tri- and tetrasubstituted alkene dipeptide mimetics to conformational studies of cyclic RGD peptides

Shinya Oishi,[a,b] Kazuhide Miyamoto,[a] Ayumu Niida,[a] Mikio Yamamoto,[c] Keiichi Ajito,[c] Hirokazu Tamamura,[a] Akira Otaka,[a] Yoshihiro Kuroda,[a] Akira Asai[b] and Nobutaka Fujii[a,*]

[a]*Graduate School of Pharmaceutical Sciences, Kyoto University, Sakyo-ku, Kyoto 606-8501, Japan*
[b]*Graduate School of Pharmaceutical Sciences, University of Shizuoka, Shizuoka, Shizuoka 422-8526, Japan*
[c]*Pharmaceutical Research Center, Meiji Seika Kaisha, Ltd., Kohoku-ku, Yokohama 222-0002, Japan*

Received 4 October 2005; revised 13 November 2005; accepted 15 November 2005

Available online 6 December 2005

Abstract—The first application of a combination of novel ψ[(*E*)-CX=CX]-type alkene dipeptide isosteres to conformation studies of cyclic bioactive peptides was carried out (X=H or Me). For exploration of bioactive conformations of Kessler's cyclic RGD peptides, cyclo(-Arg-Gly-Asp-D-Phe-Val-) **1** and cyclo(-Arg-Gly-Asp-D-Phe-*N*-MeVal-) **2**, D-Phe-ψ[(*E*)-CX=CX]-L-Val-type dipeptide isosteres were utilized having di-, tri- and tetrasubstituted alkenes containing the γ-methylated isosteres that have been reported to be potential type II′ β-turn promoters. All of the (*E*)-alkene pseudopeptides **3–6** exhibited higher antagonistic potency against $\alpha_v\beta_3$ integrin than **1**, although potencies were slightly lower than **2**. Detailed structural analysis using ^{1}H NMR spectroscopy revealed that representative type II′ β/γ backbone arrangements proposed for **1**, were not observed in peptides **3–6**. Rather on the basis of ^{1}H NMR data, the conformations of peptides **3–6** were estimated to be more analogous to those of the *N*-methylated peptide **2**.

1. Introduction

Use of both natural and artificial modifications of bioactive peptides and proteins provides opportunities to better understand the basis for bioactivities of the parent structures and to find novel functionality that may be applied for new purposes.[1] Application of unnatural amino acids and peptidomimetics constitutes one of the most powerful methodologies in such chemical approaches to understanding ligand–protein interactions.[2] Among large numbers of mimetics, (*E*)-alkene dipeptide isosteres that are designed as nonpolar alkene replacements of planar amide moieties within dipeptides, have been widely applied to bio- and chemoactive peptides by us and others (Fig. 1).[3] Gellman et al. reported that Gly-ψ[(*E*)-CMe=CMe]-Gly-type isostere **D** is a potential β-hairpin promoter.[4] In addition, Wipf et al. have characterized D-Ala-ψ[(*E*)-CMe=CH]-L-Ala- and L-Ala-ψ[(*E*)-CCF_3=CH]-D-Ala-type isosteres such as **C** as promoting β-turn formation in the solid state due to $A^{1,2}$- and $A^{1,3}$-strain as opposed to L-Ala-ψ[(*E*)-CH=CH]-D-Ala-type motifs exemplified by **A** that have a disubstituted alkene.[5] These γ-methylated and γ-trifluoromethylated isosteres, which possess a carbon atom corresponding to a peptide bond carbonyl oxygen, are thought to be reasonable amide mimetics. Recent development of organocopper-mediated stereoselective synthesis of multi-substituted (*E*)-alkene isosteres[6] allowed us to utilize a combination of these isosteres for practical structure–activity relationship (SAR) studies on bioactive peptides.[5,6]

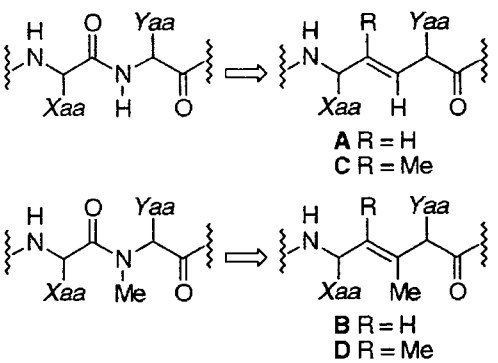

Figure 1. (*E*)-Alkene dipeptide isosteres having di-, tri- and tetrasubstituted alkenes; Xaa, Yaa = amino acid side chains.

As an exemplary application, we chose cyclic RGD peptides, cyclo(-Arg-Gly-Asp-D-Phe-Val-) **1**[7] and cyclo(-Arg-Gly-Asp-D-Phe-*N*-MeVal-) **2**,[8] which have

Keywords: (*E*)-Alkene dipeptide isostere; Cyclic RGD peptide; Integrin; Structure–activity relationship study.
* Corresponding author. Tel.: +81 75 753 4551; fax: +81 75 753 4570; e-mail: nfujii@pharm.kyoto-u.ac.jp

0040–4020/$ - see front matter © 2005 Elsevier Ltd. All rights reserved.
doi:10.1016/j.tet.2005.11.033

been shown to be highly potent and selective $\alpha_v\beta_3$ integrin antagonists (Fig. 2). It is well-known that $\alpha_v\beta_3$ integrin receptor and its ligands participate in many biological processes including tumor-induced angiogenesis and adhesion of osteoclasts to bone matrix and so on.[9] Peptide **1** was originally reported to adopt two distinctive secondary structures in DMSO solution; a type II′ β-turn with D-Phe at the $i+1$ position and a γ-turn with Gly at the $i+1$ position.[10,11] These structures allow two principal pharmacophores consisting of an Arg guanidino group and an Asp carboxylic acid to be located in close proximity. Among cyclic peptides, **2** is the most potent $\alpha_v\beta_3$ antagonist reported so far. It has been found to exhibit considerable conformational flexibility in water, including interconversion of two inverse γ turns (γ_i turns) and a γ turn, that do not afford identical topology of two closely located pharmacophores as observed in **1**.[8] On the other hand, the binding structure of **2** with $\alpha_v\beta_3$ integrin, which was recently disclosed by a crystal structure analysis of the ligand–receptor complex, is somewhat different from that proposed by Kessler et al.[12] The ligand binding seems to induce a structural change of the ligand binding domains of $\alpha_v\beta_3$ intergin, as well as a conformation change of ligand itself. As a result, peptide **2** exhibits distorted backbone conformations in the binding state to some extent, as compared with its calculated free-state conformations. Meanwhile, addition of an *N*-methyl group to the Val residue apparently improves $\alpha_v\beta_3$ antagonistic activity and $\alpha_v\beta_3/\alpha_{IIb}\beta_3$ selectivity, while the effect of *N*-methylation on the conformation of peptides as a whole as well as on the topology of the pharmacophores, especially in the neighbourhood of the D-Phe-Val/MeVal peptide bond, have not been discussed in detail. As such, it is difficult to rationalize structural and biological effects of certain characteristic functional groups in spite of such extensive research.

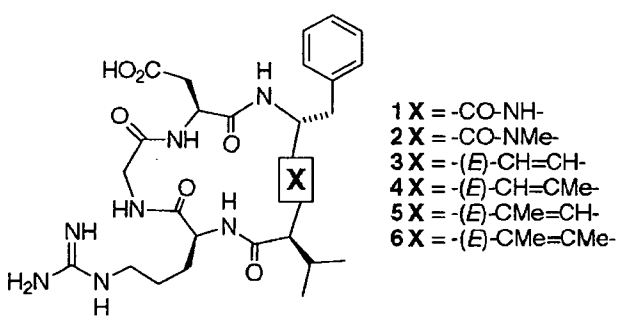

Figure 2. Structures of cyclic RGD peptides and peptidomimetics.

We recently reported the diastereoselective synthesis of γ-unmethylated D-Phe-ψ[(*E*)-CH=CX]-L-Val- and D-Phe-ψ[(*Z*)-CH=CMe]-L-Val-type alkene dipeptide isosteres (X=H or Me) with application to D-Phe-L-Val/*N*-MeVal moieties in peptides **1** and **2**.[6b] Both peptides **3** and **4** contain ψ[(*E*)-CH=CH]- and ψ[(*E*)-CH=CMe]-type isosteres, respectively, and exhibit potent antagonistic activity against $\alpha_v\beta_3$ integrin. In contrast, (*Z*)-congeners show extremely low $\alpha_v\beta_3$ and $\alpha_{IIb}\beta_3$ antagonist potency. This indicated that cis-conformation within the D-Phe-L-Val/*N*-MeVal peptide bond distorted the peptide bioactive conformations. On the other hand, slight differences between the potencies of **3** and **4**, which are independent of the presence of a β-methyl group in **4** that corresponds to an *N*-methyl group of **2**, support a conformational role for the *N*-methyl group of **2** beyond a simple steric one. To facilitate a deeper understanding of structure–activity relationships of cyclic RGD peptides, it was thought that utilization of highly functional β-turn promoters such as γ-methylated (*E*)-alkene isosteres, could be of value. Moreover, a D-Phe-ψ[(*E*)-CMe=CMe]-L-Val-type analogue could also be regarded as a D-Phe-L-*N*-MeVal dipeptide equivalent having reduced polarity, wherein the β- and γ-methyl groups could replicate allylic strain across peptide bonds between the D-Phe carbonyl oxygen and the *N*-MeVal side chain, as well as between the *N*-methyl group and the D-Phe side chain.[13] With this in mind, the synthesis and bio-evaluation of isostere-containing cyclic peptides **5** and **6** was undertaken, along with ^{1}H NMR conformational analysis and comparison with the previous peptides **1–4**. Reported herein are results of our application of γ-methylated alkene dipeptide isosteres to proposed type II′ β-turn motifs in bioactive peptides. We also examined the structure–activity effects of *N*-methylation of Val in cyclic RGD peptides using (*E*)-alkene isosteres having differential substitution motifs.

2. Results and discussion

2.1. Synthesis

Preparation of cyclic RGD peptides **5** and **6** that contain D-Phe-ψ[(*E*)-CMe=CH]-L-Val- and D-Phe-ψ[(*E*)-CMe=CMe]-L-Val-type alkene dipeptide isosteres, respectively, was performed according to the synthetic scheme utilized for the synthesis of peptide **4** (Schemes 1 and 2).[6b] In this process, a combination of Fmoc-based solid phase peptide synthesis (SPPS) and cyclization of linear peptide

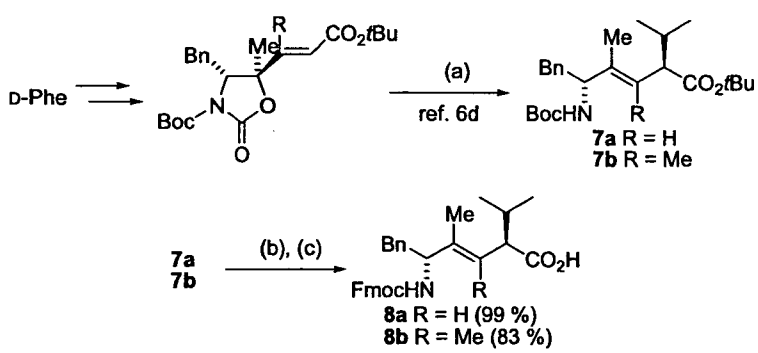

Scheme 1. (a) Organocopper reagents; (b) TFA; (c) Fmoc-OSu, Et_3N.

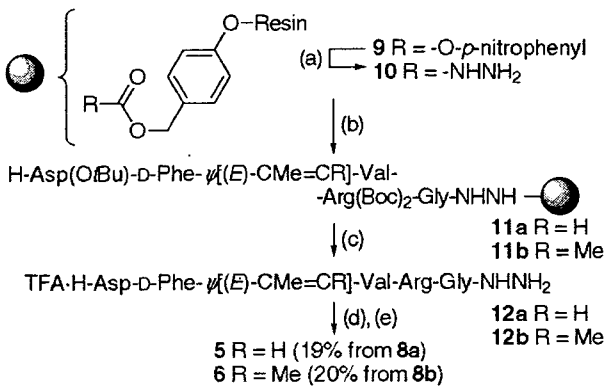

Scheme 2. (a) $NH_2NH_2 \cdot H_2O$; (b) Fmoc-based SPPS; (c) TFA; (d) HCl, isoamyl nitrite; (e) $i Pr_2NEt$.

hydrazides **12a,b** without side-chain protecting groups was employed by an adapted azide method in order to avoid olefinic isomerization, which would otherwise be possible during final deprotection by strong acid treatment in Boc-based synthesis. For side-chain protection, *tert*-butyl ester for Asp and $(Boc)_2$ for Arg were employed, both of which are amenable to mild acidic deprotection. TFA-treatment of the *N*-Boc-protected isosteres **7a,b**, which were obtained by regio- and stereoselective alkylation of β-(1,3-oxazolidin-2-one)-5-yl-α,β-enoates by organocopper reagents,[14] followed by Fmoc-reprotection, provided building blocks **8a,b** that were suitable for SPPS. Following the preparation of hydrazide linker **10** by treatment of *p*-nitrophenyl carbonate resin **9** with hydrazine hydrate in DMF, peptide chain elongation by Fmoc-based SPPS gave the expected protected peptide resins **11a,b**. Side chain deprotection and TFA-mediated cleavage from resins **11a,b** provided peptide hydrazides **12a,b**, which were subjected to successive azide formation and cyclization in highly diluted DMF solution.[15] The crude peptides were readily purified by reverse-phase HPLC to yield the expected cyclic peptides **5** and **6** in 19 and 20% yield, respectively, which were fully characterized by ^1H NMR and mass spectra.

2.2. Structure–activity relationships of cyclic RGD peptides and peptidomimetics

Integrin antagonistic activities of the resulting peptides **5** and **6** against $\alpha_v\beta_3$ and $\alpha_{IIb}\beta_3$ integrins were comparatively evaluated along with Kessler's RGD peptides **1** and **2**, and peptides **3** and **4** having γ-unmethylated D-Phe-ψ[(*E*)-CH=CX]-L-Val-type isosteres (X=H or Me). ELISA assays were performed using immobilized $\alpha_v\beta_3$ or $\alpha_{IIb}\beta_3$ integrin, according to the modified method of Kouns et al.[16] The results are shown in Table 1 as inhibition by peptides **1–6** of vitronectin or fibrinogen binding to the respective integrins ($n=8$). Each of the isostere-containing peptides **3–6** showed strong $\alpha_v\beta_3$ integrin antagonistic activity within the range from $IC_{50}=6.8$ nM for **1** to $IC_{50}=1.4$ nM for **2**. It appeared that the amide or olefinic moiety in the D-Phe-Val/*N*-MeVal dipeptide portion of peptides **1–6** was not directly involved in recognition and binding to $\alpha_v\beta_3$ integrin. These data also support that *trans*-amide conformation within the D-Phe-Val/*N*-MeVal dipeptide was predominant in the bioactive conformations. This is consistent with a crystal structure analysis of an $\alpha_v\beta_3$ integrin–ligand complex[12] and our previous research using a combination of (*E*)- and (*Z*)-alkene dipeptide isosteres.[6b] Structure–activity relationship studies on cyclic RGD peptides investigating effects due to the *N*-methyl group of **2** using novel alkene dipeptide isosteres seemed to be highly appropriate.

It is noteworthy that only minimal differences were observed between the activities of peptides **3** and **5** having β-unmethylated isosteres and the respective β-methylated isostere-containing congeners **4** and **6**. In contrast, peptide **2**, having *N*-methyl valine, exhibited approximately five times higher potency than peptide **1**, similar to a previous report.[8] If *N*-methylation is potency-enhancing in **2**, then either peptide **4** or **6**, which possesses β-methyl group isosteric to the *N*-methyl group of **2**, could also show potencies superior to **3** or **5**, respectively. This unexpected result demonstrated that a conformational transformation from **1** to **2** and the resulting improvement of $\alpha_v\beta_3$ integrin antagonism depend on factors other than simple steric properties of the *N*-methyl group.

It was also found that peptides **5** and **6**, containing an isostere γ-methyl group, had slightly higher potency against $\alpha_v\beta_3$ integrin than the γ-unmethylated congeners **3** and **4**, respectively. Interestingly, in a crystal structure of peptide **2** complexed to $\alpha_v\beta_3$ integrin, the carbonyl oxygen of D-Phe, to which the isostere γ-methyl group corresponds, is not directly associated with any polar interactions with integrin, such as hydrogen bonding.[12] In light of this, the improved potencies of **5** and **6** may potentially be derived from steric interactions, including allylic strain induced by the γ-methyl group. Similarly, it could be surmised that D-Phe carbonyl oxygens of **1** and **2** could partially contribute to

Table 1. Integrin antagonistic activities of cyclic RGD peptides and peptidomimetics

Peptide	X	$\alpha_v\beta_3$		$\alpha_{IIb}\beta_3$		SI[a]
		IC_{50} (nM)[b]	Q[c]	IC_{50} (nM)[b]	Q[c]	
RGDS[d]	—	98±29	14	270±41	0.35	2.7
1	–CO–NH–	6.8±2.7	1	770±120	1	110
2	–CO–NMe–	1.4±0.31	0.20	280±42	0.36	200
3	–CH=CH–	3.6±1.3	0.53	140±18	0.19	40
4	–CH=CMe–	3.3±0.93	0.48	100±42	0.13	30
5	–CMe=CH–	2.4±0.33	0.35	81±18	0.11	34
6	–CMe=CMe–	1.8±0.51	0.27	48±11	0.06	26

[a] SI values were calculated as $SI=IC_{50}(\alpha_{IIb}\beta_3)/IC_{50}(\alpha_v\beta_3)$.
[b] The data for peptides **1–6** were obtained in comparative experiments using the same conditions.
[c] *Q* values were calculated as $Q=IC_{50}(\text{peptide})/IC_{50}(\mathbf{1})$.
[d] A linear peptide RGDS (H-Arg-Gly-Asp-Ser-OH) was used as a standard peptide.

appropriate dispositions of close functional groups, resulting in enhanced potencies.

In contrast, isostere-containing peptides **3–6** were less selective $\alpha_v\beta_3$ integrin antagonists than **1** or **2**, due to their relatively high potency against $\alpha_{IIb}\beta_3$ integrin. These increased potencies against $\alpha_{IIb}\beta_3$ integrin resulted from substituting the amide bonds of **1** and **2** with alkene isosteres, indicated that distinct functional groups derived from the olefinic moieties may be compatible with structural features of $\alpha_{IIb}\beta_3$ integrin. Other independent factors of RGD motifs displayed by the ligands may contribute to selectivity in interaction with the two integrins. However, we failed to ascertain what characteristics could be associated with selective recognition by the respective integrins. Locardi et al. revealed that the conformations of $\alpha_{IIb}\beta_3$ antagonists are different in the presence and absence of the receptor.[17] It is conceivable that the cyclic peptides may vary their shape by distinctive interactions in the binding state, even if the isostere moieties in **3–6** do not affect peptide conformations in the absence of the receptor.

2.3. Conformational aspects of cyclic peptidomimetics derived from ^{1}H NMR spectroscopy

Conformations of cyclic peptides have been intensively investigated using NMR spectroscopy and molecular dynamics calculations.[18] In structure–activity relationship studies on cyclic RGD peptides under 'conformational control', Kessler et al. reported that replacement at either the D-Phe or Val positions did not induce changes in backbone conformations.[10a] ^{1}H NMR parameters such as chemical shifts, temperature dependence of amide protons and ^3J-coupling constants support homogeneous families of cyclic peptide conformations. Based on similar concepts using alkene isosteres, we attempted to understand effects of the *N*-methyl groups or isostere β-methyl groups on conformations and their relationship to $\alpha_v\beta_3$ integrin antagonistic activity.[19]

In chemical shift data of peptides **1–6** in DMSO solution, downfield shifts of Arg H^N, Asp H^N, one Gly H^α (high field) and D-Phe H^α of peptides **2**, **4** and **6** that possess *N*-MeVal *N*-methyl groups or corresponding β-methyl groups, were comparable to those of **1**, **3** and **5**, respectively, (see the Supporting information). On the other hand, Gly H^N, Arg H^α, the other Gly H^α (low field) and Asp H^α of **2**, **4** and **6** were located at higher fields than those of **1**, **3** and **5**, respectively. For D-Phe H^N, no significant differences were found between **1** and **2**, while similar upfield shift correlations were observed among the isostere-containing peptides **3–6**. As such, the addition of a methyl group to the α-amino group of Val or to the isostere β-position, induced nearly equal chemical shift changes, although this may not necessarily indicate similar changes in peptide backbone conformation. These observations are in contrast to the fact that among peptides **2**, **4** and **6**, an increase in $\alpha_v\beta_3$ integrin antagonistic activity was observed only in **2**.

In a sharp contrast to effects on the chemical shifts of amide and α-protons, the vicinal coupling constants between amide protons and α-protons of each residue of peptides **1–6** displayed no common tendency due to *N*-methylation or β-methylation. If anything, the values of each residue were similar among all the peptides **1–6**. This revealed that methylation did not result in drastic ϕ angle changes.

Temperature coefficients often indicate solvent accessibility of amide protons.[18a] Kessler et al. previously reported that the temperature dependence of Arg H^N in cyclo(-Arg-Gly-Asp-D-Xaa^4-Val-) and cyclo(-Arg-Gly-Asp-D-Phe-Yaa^5-) is typically small, except in cases where cyclic amino acids such as proline are utilized for D-Xaa^4 and Yaa^5.[10a] This data supports solvent shielding of Arg H^N and indicates the presence of a hydrogen bond corresponding to a type II′ β-turn substructure. On the other hand, only a small coefficient for Gly H^N is observed in peptide **2**, although it has been reported that this has no relation to hydrogen bonding.[8] If anything, peptide **2** appeared to exhibit conformational flexibility around the Gly residues. We examined this parameter comparatively in peptides **1–6**, based on chemical shifts of amide protons in the range of 300–340 K (Table 2). Interestingly, among peptides **1–6**, a small coefficient for Arg H^N was observed in peptide **1** only, while the Gly H^N coefficients were small in the remaining peptides **2–6**. Coefficients of other residues in **2–6** were over 2.0 ppb/K, although these varied somewhat for residue among the peptides. Thus, temperature dependence tendencies of amide protons in isostere-containing peptides **3–6** appeared to be nearly identical with **2**, but different from **1**. These observations implied that the conformations of **3–6** may resemble one another in DMSO, and that these peptides may adopt flexible structures similar to **2**, rather than the representative type II′ β/γ arrangements seen with **1**.

Table 2. Temperature dependence of amide proton chemical shifts, $-\Delta\delta/\Delta T$ (ppb/K) of cyclic peptides **1–6**[a]

Peptide	Arg	Gly	Asp	D-Phe	Val
1	1.8	5.5	5.1	3.1	3.0
2	5.5	1.0	4.7	5.1	—
3	5.4	2.2	3.0	3.5	—
4	4.8	0.9	5.5	3.3	—
5	5.7	2.5	5.5	2.7	—
6	6.8	−1.4	7.4	2.5	—

[a] The data for peptides **1–6** were obtained in comparative experiments using the same conditions.

Taking into account combined biological and ^{1}H NMR data, it is evident that the lack of a Val amide hydrogen incurred by *N*-methylation in **2**, may have contributed to conformational changes that increased $\alpha_v\beta_3$ antagonistic activity. This was also observed with peptides **3–6** having alkene isosteres as well. In other words, the Val amide proton in **1** may contribute unfavorably to bioactive conformations likely through intramolecular interactions, although such an amide proton originating from the $i+2$ residue of a β-turn would be indispensable for the distinctive type II′ β/γ arrangement of cyclic pentapeptides. In contrast, it can be supposed that the carbonyl oxygen of D-Phe in **1** and **2** may be unrelated to significant interactions, since it has little apparent effect on conformation and bioactivity as compared to the amide proton of Val.

2.4. Structural calculations on cyclic peptidomimetics

To promote a better understanding of conformational aspects derived from ^{1}H NMR parameters, structural

calculations of the cyclic peptides **1–6** were carried out by simulated annealing molecular dynamics/energy minimization using dihedral constraints derived from ^{1}H NMR vicinal coupling constants and NOE distance constraints.[20] These calculations afforded well-converged conformations. Interestingly, calculated low-energy backbone structures of **1–6** are highly similar to each other (see Supporting information). Backbone structures based on the five α-carbons showed nearly symmetrical pentagonal shapes. In all cases, the olefinic moieties and peptide bonds were found to be vertical to the cyclic peptide plane, although some exhibited slightly differential rotations. Of note, the proposed type II′ β/γ arrangement of **1** was not observed in either **2–6** or in **1** itself. This apparently reflects the fact that similar averaged parameters were used for structural calculations, as reported results by Nikiforovich et al.[11] This may indicate that it could be difficult to rationalize SAR studies on cyclic RGD peptides solely using structural calculation, unless the receptor-binding structures of ligands could be discussed. In practice, the presence of β- and/or γ-methyl groups in the isostere moiety appear to have little effect on the global backbone structures of the cyclic peptidomimetics, in spite of the fact that peptides **3–6** exhibited somewhat different bioactivities, respectively.

Ten superimposed low-energy structures of peptide **6** having the D-Phe-ψ[(*E*)-CMe=CMe]-L-Val-type isostere are depicted in Figure 3 as representative of the isostere-containing peptides **3–6**. Peptide **6** was the most potent $\alpha_v\beta_3$ integrin antagonist among **3–6**. The root mean square deviation (RMSD) value for all backbone heavy atoms of **6** was below 0.22 Å, and the total energy values of the refined structures were in the range of 102–108 kcal/mol. The olefinic plane of the isostere was perpendicular to the plane of the cyclic peptide. This is an ideal substructural component for a type II′ β-turn. In practice, the averaged dihedral ψ angle of D-Phe (−103.5°) and φ angle of Val (−92.9°), were highly consistent with theoretical β-turn values. However, the expected β-turn hydrogen bond between the amide hydrogen of Arg and the α-carbonyl oxygen of Asp could not be identified, since the peptide bonds of Asp-D-Phe and Val-Arg were also oriented perpendicular to the cyclic peptide plane. The torsional angles, D-Phe φ and Val ψ, were apparently different from

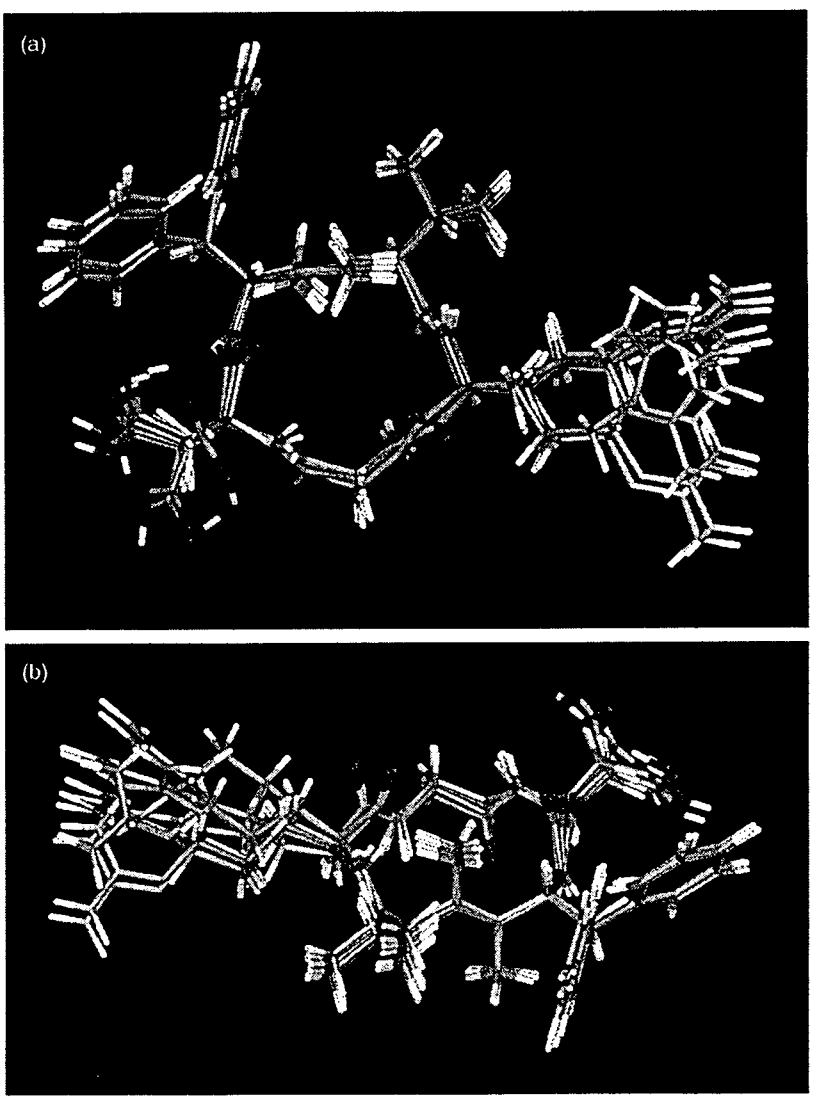

Figure 3. Overlay of ten low-energy structures of peptide **6**. (a) Top view. (b) Side view.

those typically associated with a β-turn. This allows the side chains of all residues to exhibit pseudoequatorial conformations as derived from the conformational analysis of the peptide **2**.[8] Additionally, all isostere carbonyl oxygens and γ-methyl groups were commonly directed away from side chains of neighboring residues, most probably to avoid 1,3-allylic strain across the peptide bonds. Similarly, isostere β-methyl groups were oriented upward so as to reduce steric interactions with D-Phe side chains. The averaged distance between the β-carbons of Arg and Asp of **6**, which provides topological orientation for two significant pharmacophores needed for bioactivity, was 9.0 Å. This distance was slightly longer than observed in **2**, which had previously been determined in aqueous solution.[8] These results indicated that the calculated conformation of **6** is more similar to that of the most potent peptide **2** having an *N*-methylvaline, rather than the proposed kinked conformation of **1**, which is based on a type II′ β/γ conformation.[21]

In $\alpha_v\beta_3$ integrin–ligand complexes, ligand **2** was reported to adopt a more distorted conformation as compared with structures in the absence of integrin.[12] In addition, it has been shown recently that cyclic RGD peptide ligands vary in conformations in the presence of integrins.[17,23] Thus, it may be of significance to discuss the effects of the D-Phe-L-Val/*N*-MeVal moieties in **1–6** from the viewpoint of receptor-binding conformations, even if these moieties do not interact directly with the $\alpha_v\beta_3$ integrin in the crystal structure. Analyses of binding modes of **3–6** were not carried out. However, analogous conformations in the receptor-free state and the presence of common functional groups required for binding interactions, with the exception of the olefinic moiety, could enable an estimation of conformations of the most potent isostere-containing peptide **6** in the bound state. This presupposes that **6** can adhere to $\alpha_v\beta_3$ integrin in a manner conformationally similar to **2**.

3. Conclusion

In conclusion, SAR studies on cyclic RGD peptides were conducted using novel alkene dipeptide isosteres. Cyclic peptides **5** and **6**, having D-Phe-ψ[(*E*)-CMe=CH]-L-Val- and D-Phe-ψ[(*E*)-CMe=CMe]-L-Val-type isosteres were designed and synthesized in order to investigate effects of the type II′ β/γ arrangement found in **1** as well as the role of the *N*-methyl group of *N*-MeVal in **2** on conformation and biological activity. Evaluation of the biological activities of **1–6** against $\alpha_v\beta_3$ and $\alpha_{IIb}\beta_3$ integrin demonstrated that loss of the amide proton of Val in **1** by *N*-methylation led to a remarkable increase in $\alpha_v\beta_3$ antagonistic activity of **2**, though this was not apparently due to steric factors arising from the methyl group. Structural analysis showed that γ-methylated isostere moieties would not be expected to serve as β-turn promoters, at least in these cyclic pentapeptides. Nevertheless, the calculated conformations of isostere-containing peptides **3–6** appeared to be analogous to those reported for the most potent peptide **2** rather than for **1**. Taken together, these results indicate that influences of the *N*-methyl group on conformation and biological activity of **2** could be attributed mainly to loss of the amide hydrogen functionality in the D-Phe-*N*-MeVal moiety, as opposed to steric factors such as allylic strain induced by the methyl group.

With advances in genome science, development of efficient methodologies for the rational design of therapeutically relevant agents from natural ligands is an area of increasing importance. As presented herein, alkene isosteres having differential methyl-substitutions could serve as practical tools to derive information concerning pharmacophores and bioactive conformations of bio- and chemoactive peptides and proteins.

4. Experimental

4.1. General synthetic

^{1}H NMR spectra were recorded using a Bruker AC 300 or a Bruker AM 600 spectrometer at 300 or 600 MHz. Chemical shifts of the compounds measured in $CDCl_3$ are reported in parts per million downfield from internal Me_4Si (s= singlet, d= doublet, dd = double doublet, t= triplet, m= multiplet). Those of the compounds measured in DMSO-d_6 are calibrated to the solvent signal (2.50 ppm). Nominal (LRMS) and exact mass (HRMS) spectra were recorded on a JEOL JMS-01SG-2 or JMS-HX/HX 110A mass spectrometer. Optical rotations were measured with a Horiba high-sensitive polarimeter SEPA-200 (Kyoto, Japan). For flash chromatographies, silica gel 60H (silica gel for thin-layer chromatography, Merck) and Wakogel C-200 (silica gel for column chromatography) were employed. For HPLC separations, a Cosmosil 5C18-ARII analytical (4.6×250 mm, flow rate 1 mL/min) column or a Cosmosil 5C18-ARII preparative (20×250 mm, flow rate 11 mL/min) column was employed, and eluting products were detected by UV at 220 nm. A solvent system consisting of 0.1% TFA solution (v/v, solvent A) and 0.1% TFA in MeCN (v/v, solvent B) were used for HPLC elution.

4.1.1. (2*R*,5*R*,3*E*)-5-(9-Fluorenylmethoxycarbonyl)-amino-2-isopropyl-4-methyl-6-phenylhex-3-enoic acid (Fmoc-D-Phe-ψ[(*E*)-CMe=CH]-L-Val-OH, 8a). After treatment of the ester **7a** (108 mg, 0.258 mmol) with TFA (5 mL) for 1.5 h at room temperature, concentration under reduced pressure gave an oily residue. To a stirred solution of the above residue in MeCN–H_2O (2/1, 2.25 mL) were added Et_3N (0.072 mL, 0.517 mmol) and a solution of Fmoc-OSu (91 mg, 0.271 mmol) in MeCN (1.5 mL) at 0 °C. After being stirred for 3 h, the mixture was acidified with 0.1 N HCl and was extracted with EtOAc. The extract was washed with 0.1 N HCl and brine, and dried over $MgSO_4$. Concentration under reduced presssure followed by flash chromatography over silica gel with *n*-hexane–EtOAc (2/1) gave the title compound **8a** (123 mg, 99% yield) as a colorless oil: $[\alpha]_D^{20}$ −16.6 (*c* 0.542 in $CHCl_3$); ^{1}H NMR (300 MHz, $CDCl_3$, 55 °C, TMS): δ 0.70 (d, *J*=6.7 Hz, 3H), 0.87 (d, *J*=6.6 Hz, 3H), 1.67 (s, 3H), 1.92 (m, 1H), 2.77–2.99 (m, 3H), 4.14 (t, *J*=6.6 Hz, 1H), 4.25–4.41 (m, 3H), 4.91 (m, 1H), 5.26 (d, *J*=10.1 Hz, 1H), 7.08 (d, *J*=6.9 Hz, 2H), 7.12–7.30 (m, 5H), 7.35 (t, *J*=7.4 Hz, 2H), 7.49 (m, 2H), 7.72 (d, *J*=7.5 Hz, 2H). LRMS (FAB), *m/z* 484 (MH^+), 392, 260, 191, 179, 164, 154, 149, 143, 136,

91, 57, 43. HRMS (FAB), *m/z* calcd for $C_{31}H_{34}NO_4$ (MH^+) 484.2488, found: 484.2477.

4.1.2. (2*R*,5*R*,3*E*)-5-(9-Fluorenylmethoxycarbonyl)-amino-2-isopropyl-3,4-dimethyl-6-phenylhex-3-enoic acid (Fmoc-D-Phe-ψ[(*E*)-CMe=CMe]-L-Val-OH, 8b). By use of a procedure similar to that described for the preparation of the Fmoc-amino acid **8a** from **7a**, the ester **7b** (138 mg, 0.319 mmol) was converted into the title compound **8b** (131 mg, 83% yield) as a colorless oil: $[\alpha]_D^{24}$ −70.9 (*c* 1.00 in $CHCl_3$); ^1H NMR (300 MHz, $CDCl_3$, 50 °C, TMS) δ 0.36 (m, 3H), 0.91 (d, *J*=6.4 Hz, 3H), 1.49 (m, 3H), 1.71 (d, *J*=1.4 Hz, 3H), 1.96 (m, 1H), 2.66 (m, 1H), 2.81 (m, 1H), 3.98 (m, 1H), 4.15 (t, *J*=6.4 Hz, 1H), 4.41 (m, 2H), 4.81 (br, 1H), 7.06 (br, 2H), 7.10–7.30 (m, 5H), 7.31–7.39 (m, 2H), 7.51 (m, 2H), 7.72 (m, 2H). LRMS (FAB), *m/z* 498 (MH^+, base peak), 452, 406, 391, 274, 191, 179, 149, 136, 91, 69, 57, 43. HRMS (FAB), *m/z* calcd for $C_{32}H_{36}NO_4$ (MH^+) 498.2644, found: 498.2641.

4.2. General procedure for assembly of the peptide chain

Protected peptide resins were manually constructed by Fmoc-based solid phase peptide synthesis. *t*Bu ester for Asp and $(Boc)_2$ for Arg were employed for side-chain protection. Fmoc-amino acids except for Fmoc-D-Phe-ψ[(*E*)-CMe=CX]-Val-OH (X=H or Me) were coupled using 5 equiv of reagents [Fmoc-amino acid, *N*,*N*′-diisopropylcarbodiimide (DIPCDI), and HOBt·H_2O] to free amino group (or hydrazino group) in DMF for 1.5 h. Fmoc deprotection was performed by 20% piperidine in DMF (2×1 min, 1×20 min).

4.2.1. H-Asp(O*t*Bu)-D-Phe-ψ[(*E*)-CMe=CH]-Val-Arg(Boc)$_2$-Gly-NHNHCO-Wang resin (11a). After treatment of *p*-nitrophenyl carbonate Wang resin **9** (0.93 mmol g^{-1}, 161 mg, 0.15 mmol) with $NH_2NH_2 \cdot H_2O$ (0.046 mL, 0.75 mmol) in DMF (2 mL) at room temperature for 2 h, Gly and $Arg(Boc)_2$ residues were coupled by general coupling protocol. Fmoc-D-Phe-ψ[(*E*)-CMe=CH]-Val-OH **8a** (48.3 mg, 0.100 mmol) was incorporated by double treatment with DIPCDI (0.018 mL, 0.120 mmol) and HOBt·H_2O (0.015 mg, 0.100 mmol) for 1.5 h each. After capping of the remaining free amino group with Ac_2O–pyridine, Asp(O*t*Bu) residue was coupled by general coupling protocol to provide the title peptide resin **11a**.

4.2.2. H-Asp(O*t*Bu)-D-Phe-ψ[(*E*)-CMe=CMe]-Val-Arg(Boc)$_2$-Gly-NHNHCO-Wang resin (11b). By use of a procedure similar to that described for the preparation of the resin **11a**, the title resin **11b** was synthesized from *p*-nitrophenyl carbonate Wang resin **9** (0.15 mmol) and Fmoc-amino acid **8b** (60 mg, 0.121 mmol).

4.2.3. Cyclo[-Arg-Gly-Asp-D-Phe-ψ[(*E*)-CMe=CH]-Val-]·TFA (5). The protected peptide resin **11a** was treated with TFA for 1.5 h at room temperature. Removal of the resin followed by concentration under reduced pressure gave the colorless residue, which was purified by preparative HPLC (linear gradient of B in A, 15–20% over 45 min) to provide a peptide hydrazide **12a**. To a stirred solution of **12a** in DMF (12 mL) were added a solution of 4 M HCl in DMF (0.075 mL, 0.300 mmol) and isoamyl nitrite (0.013 mL, 0.100 mmol) at −40 °C, and the mixture was stirred for 30 min at −20 °C. After dilution of the mixture with precooled DMF (68 mL), iPr$_2$NEt (0.174 mL, 1.00 mmol) was added at −40 °C, and the mixture was stirred for 24 h at −20 °C. Concentration under reduced pressure and purification by preparative HPLC (linear gradient of B in A, 20–25% over 30 min) to give the cyclic pseudopeptide **5** (13.1 mg, 19% yield from **8a**) as freeze-dried powder: $[\alpha]_D^{20}$ −59.4 (*c* 0.656 in H_2O); t_R= 33.4 min (linear gradient of B in A, 20–40% over 40 min); ^1H NMR (600 MHz, DMSO-d_6, 25 °C) δ 0.46 (d, *J*=6.6 Hz, 3H), 0.66 (d, *J*=6.6 Hz, 3H), 1.32–1.46 (m, 2H), 1.53 (m, 1H), 1.58 (s, 3H), 1.69 (m, 1H), 1.84 (m, 1H), 2.40 (dd, *J*=16.2, 6.7 Hz, 1H), 2.56 (t, *J*=9.1 Hz, 1H), 2.66 (dd, *J*=16.2, 7.8 Hz, 1H), 2.74 (dd, *J*=13.5, 9.7 Hz, 1H), 2.84 (dd, *J*=13.5, 5.8 Hz, 1H), 3.07 (m, 2H), 3.26 (dd, *J*=14.4, 4.2 Hz, 1H), 3.98 (dd, *J*=14.4, 6.8 Hz, 1H), 4.17 (m, 1H), 4.29 (m, 1H), 4.55 (m, 1H), 5.05 (d, *J*=9.4 Hz, 1H), 7.12–7.25 (m, 5H), 7.36 (d, *J*=8.3 Hz, 1H), 7.46 (m, 1H), 7.93–7.99 (m, 2H), 8.11 (d, *J*=8.3 Hz, 1H), 12.28 (br, 1H). LRMS (FAB), *m/z* 572 (MH^+), 185, 154, 137, 93. HRMS (FAB), *m/z* calcd for $C_{28}H_{42}N_7O_6$ (MH^+) 572.3197, found: 572.3208.

4.2.4. Cyclo[-Arg-Gly-Asp-D-Phe-ψ[(*E*)-CMe=CMe]-Val-]·TFA (6). By use of a procedure similar to that described for the preparation of the peptide **5** from the resin **11a**, the resin **11b** was converted into the title peptide **6** (16.9 mg, 20% yield): $[\alpha]_D^{22}$ −62.6 (*c* 0.846 in H_2O); t_R= 36.3 min (linear gradient of B in A, 20–40% over 40 min); ^1H NMR (600 MHz, DMSO-d_6, 25 °C) δ 0.26 (d, *J*=6.5 Hz, 3H), 0.80 (d, *J*=6.4 Hz, 3H), 1.33–1.49 (m, 5H), 1.71 (s, 3H), 1.72–1.81 (m, 2H), 1.86 (m, 1H), 2.43 (dd, *J*=16.5, 6.8 Hz, 1H), 2.70–2.79 (m, 3H), 2.84 (dd, *J*=13.3, 5.1 Hz, 1H), 3.07 (m, 2H), 3.27–3.32 (m, 1H), 3.86 (m, 1H), 3.91 (dd, *J*=14.4, 6.7 Hz, 1H), 4.52 (m, 1H), 4.92 (m, 1H), 7.10–7.22 (m, 5H), 7.29 (m, 1H), 7.50 (br, 1H), 7.56 (d, *J*= 6.9 Hz, 1H), 7.74 (d, *J*=7.4 Hz, 1H), 8.54 (d, *J*=8.2 Hz, 1H), 12.30 (br, 1H). LRMS (FAB), *m/z* 586 (MH^+), 154 (base peak), 93, 91, 87, 70. HRMS (FAB), *m/z* calcd for $C_{29}H_{44}N_7O_6$ (MH^+) 586.3353, found: 586.3368.

4.3. Integrin-binding assays

Compounds were evaluated for their inhibitory activities in $\alpha_v\beta_3$ and $\alpha_{IIb}\beta_3$-ELISA (enzyme linked immunosorbent assay). $\alpha_v\beta_3$ was purified from human placenta, using RGDSPK-sepharose CL-4B affinity chromatography, followed by mono Q ion exchange chromatography, according to Pytela's protocol.[24] $\alpha_{IIb}\beta_3$ was purified from human platelet by RGDSPK-sepharose CL-4B as well.[24] $\alpha_v\beta_3$ and $\alpha_{IIb}\beta_3$ binding assays were performed according to the modified method of Kouns et al.[16] EIA plates were coated with $\alpha_v\beta_3$ or $\alpha_{IIb}\beta_3$, and blocked with bovine serum albumin. In each reaction, a test sample in the reaction mixture (20 mM Tris–HCl, 150 mM NaCl, 1 mM $CaCl_2$, 1 mM $MgCl_2$, pH 7.4, 0.100 mL) including vitronectin or fibrinogen, was added to the receptor-coated plate and incubated for 4 h at 25 °C. Thereafter the ligand binding was measured using anti-vitronectin rabbit antibody and peroxidase-conjugated anti-rabbit IgG antibody for $\alpha_v\beta_3$, or peroxidase-conjugated anti-fibrinogen antibody for

$\alpha_{IIb}\beta_3$, and 2,2′-azino-bis(3-ethylbenzthiazoline-6-sulfonic acid) as the substrate of peroxidase. The IC_{50} values were determined from measurement of absorbance at 415 nm.

4.4. NMR spectroscopy

The peptide sample was dissolved in DMSO-d_6 at concentration of 5 mM. ^{1}H NMR spectra of the peptides were recorded at 300 K using a Bruker AM 600 spectrometer at 600 MHz ^{1}H frequency. The chemical shifts were referenced to the residual DMSO (2.50 ppm). The assignments of the proton resonances were completely achieved by use of ^{1}H–^{1}H COSY spectra. $^3J(H^N,H^\alpha)$ coupling constants were measured from one-dimensional spectra. The mixing time for the NOESY experiments was set at 200, 300 and 400 ms. NOESY spectra were composed of 2048 real points in the F2 dimension and 512 real points, which were zero-filled to 1024 points in the F1 dimension, with 32 scans per t1 increment. The cross-peak intensities were evaluated by relative build-up rates of the cross-peaks. For the examination of the temperature dependence of the amide protons, the spectra of all peptides were also recorded at the every 10 K in the range of 300–340 K.

4.5. Calculation of structures

The structure calculations were performed on a Silicon Graphics Origin 2000 workstation with the NMR-refine program within the Insight II/Discover package using the consistent valence force field (CVFF). The prochiralities of two γ-methyl protons of Val were assigned based on the $^3J(H^\alpha,H^\beta)$ and the different NOE intensities in the NOESY spectra. On the other hand, the pseudoatoms were defined for the methylene protons of Arg, Asp and D-Phe, prochiralities of which were not identified by ^{1}H NMR data. The restraints, in which the Gly α-methylene participated, were defined for the separate protons without definition of the prochiralities. The dihedral ϕ angle constraints were calculated based on the Karplus equation: $^3J(H^N,H^\alpha)=6.7\cos^2(\theta-60)-1.3\cos(\theta-60)+1.5$.[25] Lower and upper angle errors were set to 15°. The NOESY spectra with a mixing time of 200 ms were used for the estimation of the distance restraints between protons. The NOE intensities were classified into three categories (strong, medium and weak) based on the number of contour lines in the cross-peaks to define the upper-limit distance restraints (2.7, 3.5 and 5.0 Å, respectively). The upper-limit restraints were increased by 1.0 Å for the involved pseudoatoms. Lower bounds between nonbonded atoms were set to their van der Walls radii (1.8 Å). These restraints were included with force constants of 25–100 kcal mol^{-1} Å^{-2} for the distances and of 25–100 kcal mol^{-1} rad^{-2} for the dihedral angles. The 50 initial structures generated by the NMR refine program randomly were subjected to the simulated annealing calculations. Detailed protocols for the calculation are found in the Supporting information. The final minimization stage was achieved until the maximum derivative became less than 0.01 kcal mol^{-1} Å^{-2} by the steepest descents and conjugate gradients methods without any solvent matrix. The families of the preferred conformations were selected from the structures with energies not higher than 8 kcal mol^{-1} compared with the lowest energy.

Acknowledgements

We thank Dr. Terrence R. Burke, Jr., NCI, NIH, for reading manuscript and valuable discussions. This work was supported by Grant-in-Aid for Scientific Research from the Ministry of Education, Culture, Sports, Science, and Technology of Japan, 21st Century COE program 'Knowledge Information Infrastructure for Genome Science', and Health and Labour Sciences Research Grants (Research on HIV/AIDS). Computation time was provided by the Supercomputer Laboratory, Institute for Chemical Research, Kyoto University. S.O. is grateful for the JSPS Research Fellowships for Young Scientists.

Supplementary data

Supplementary data associated with this article can be found, in the online version, at doi:10.1016/j.tet.2005.11.033. ^{1}H NMR spectra for all new compounds; ^{1}H NMR data of **3–6**; protocols of structural calculations; calculated structures and averaged dihedral angles of **3–5**; and overlay of the representative structures of **3–6**.

References and notes

1. (a) Wang, L.; Brock, A.; Schultz, P. G. *J. Am. Chem. Soc.* **2002**, *124*, 1836–1837. (b) Chin, J. W.; Santoro, S. W.; Martin, A. B.; King, D. S.; Wang, L.; Schultz, P. G. *J. Am. Chem. Soc.* **2002**, *124*, 9026–9027.
2. For recent reviews of peptidomimetics, see: (a) Hruby, V. J.; Balse, P. M. *Curr. Med. Chem.* **2000**, *7*, 945–970. (b) Kim, H.-O.; Kahn, M. *Combi. Chem. High Throughput Screen* **2000**, *3*, 167–183. (c) Bursavich, M. G.; Rich, D. H. *J. Med. Chem.* **2002**, *45*, 541–558. (d) Freidinger, R. M. *J. Med. Chem.* **2003**, *46*, 5553–5566.
3. (a) Fujimoto, K.; Doi, R.; Hosotani, R.; Wada, M.; Lee, J.-U.; Koshiba, T.; Ibuka, T.; Habashita, H.; Nakai, K.; Fujii, N.; Imamura, M. *Life Sci.* **1997**, *60*, 29–34. (b) Miyasaka, K.; Kanai, S.; Masuda, M.; Ibuka, T.; Nakai, K.; Fujii, N.; Funakoshi, A. *J. Auton. Nerv. Syst.* **1997**, *63*, 179–182. (c) Drew, M. G. B.; Gorsuch, S.; Mann, J.; Yoshida, S. *J. Chem. Soc., Perkin Trans. 1* **1998**, 1627–1636. (d) Hart, S. A.; Etzkorn, F. A. *J. Org. Chem.* **1999**, *64*, 2998–2999. (e) Kawaguchi, M.; Hosotani, R.; Ohishi, S.; Fujii, N.; Tulachan, S. S.; Koizumi, M.; Toyoda, E.; Masui, T.; Nakajima, S.; Tsuji, S.; Ida, J.; Fujimoto, K.; Wada, M.; Doi, R.; Imamura, M. *Biochem. Biophys. Res. Commun.* **2001**, *288*, 711–717. (f) Vasbinder, M. M.; Jarvo, E. R.; Miller, S. J. *Angew. Chem., Int. Ed.* **2001**, *40*, 2824–2827. (g) Garbe, D.; Sieber, S. A.; Bandur, N. G.; Koert, U.; Marahiel, M. A. *ChemBioChem* **2004**, *5*, 1000–1003. (h) Tamamura, H.; Hiramatsu, K.; Ueda, S.; Wang, Z.; Kusano, S.; Terakubo, S.; Trent, J. O.; Peiper, S. C.; Yamamoto, N.; Nakashima, H.; Otaka, A.; Fujii, N. *J. Med. Chem.* **2005**, *48*, 380–391 and references cited therein. (i) Jenkins, C. L.; Vasbinder, M. M.; Miller, S. J.; Raines, R. T. *Org. Lett.* **2005**, *7*, 2619–2622.
4. (a) Gardner, R. R.; Liang, G.-B.; Gellman, S. H. *J. Am. Chem. Soc.* **1995**, *117*, 3280–3281. (b) Gardner, R. R.; Liang, G.-B.; Gellman, S. H. *J. Am. Chem. Soc.* **1999**, *121*, 1806–1816.

5. Wipf, P.; Henninger, T. C.; Geib, S. J. *J. Org. Chem.* **1998**, *63*, 6088–6089.
6. (a) Oishi, S.; Kamano, T.; Niida, A.; Odagaki, Y.; Tamamura, H.; Otaka, A.; Hamanaka, N.; Fujii, N. *Org. Lett.* **2002**, *4*, 1051–1054. (b) Oishi, S.; Kamano, T.; Niida, A.; Odagaki, Y.; Hamanaka, N.; Yamamoto, M.; Ajito, K.; Tamamura, H.; Otaka, A.; Fujii, N. *J. Org. Chem.* **2002**, *67*, 6162–6173. (c) Oishi, S.; Niida, A.; Kamano, T.; Odagaki, Y.; Tamamura, H.; Otaka, A.; Hamanaka, N.; Fujii, N. *Org. Lett.* **2002**, *4*, 1055–1058. (d) Oishi, S.; Niida, A.; Kamano, T.; Odagaki, Y.; Hamanaka, H.; Yamamoto, M.; Ajito, K.; Tamamura, H.; Otaka, A.; Fujii, N. *J. Chem. Soc., Perkin Trans. 1* **2002**, 1786–1793. (e) Wipf, P.; Xiao, J. *Org. Lett.* **2005**, *7*, 103–106. (f) Xiao, J.; Weisblum, B.; Wipf, P. *J. Am. Chem. Soc.* **2005**, *127*, 5742–5743.
7. Aumailley, M.; Gurrath, M.; Muller, G.; Calvete, J.; Timpl, R.; Kessler, H. *FEBS Lett.* **1991**, *291*, 50–54.
8. Dechantsreiter, M. A.; Planker, E.; Mathä, B.; Lohof, E.; Hölzemann, G.; Jonczyk, A.; Goodman, S. L.; Kessler, H. *J. Med. Chem.* **1999**, *42*, 3033–3040.
9. (a) Hood, J. D.; Cheresh, D. A. *Nat. Rev. Cancer* **2002**, *2*, 91–100. (b) Shimaoka, M.; Springer, T. A. *Nat. Rev. Drug Discov.* **2003**, *2*, 703–716.
10. (a) Haubner, R.; Gratias, R.; Diefenbach, B.; Goodman, S. L.; Jonczyk, A.; Kessler, H. *J. Am. Chem. Soc.* **1996**, *118*, 7461–7472. (b) Haubner, R.; Finsinger, D.; Kessler, H. *Angew. Chem., Int. Ed.* **1997**, *36*, 1374–1389.
11. This II′β/γ arrangements of cyclic peptides have been a subject of some debate, such as Nikiforovich et al. recently reported: Nikiforovich, G. V.; Kövér, K. E.; Zhang, W.-J.; Marshall, G. R. *J. Am. Chem. Soc.* **2000**, *122*, 3262–3273.
12. Xiong, J.-P.; Stehle, T.; Zhang, R.; Joachimiak, A.; Frech, M.; Goodman, S. L.; Arnaout, M. A. *Science* **2002**, *296*, 151–155.
13. Hoffman, R. W. *Chem. Rev.* **1989**, *89*, 1841–1860.
14. A number of other synthetic approaches to alkene dipeptide isosteres have been reported to date: see the Ref. 6, and references cited therein.
15. Honzl, J.; Rudinger, J. *Collect. Czech. Chem. Commun.* **1961**, *26*, 2333–2344.
16. Kouns, W. C.; Kirchhofer, D.; Hadvary, P.; Edenhofer, A.; Weller, T.; Pfenninger, G.; Baumgartner, H. R.; Jennings, L. K.; Steiner, B. *Blood* **1992**, *80*, 2539–2547.
17. Locardi, E.; Mattern, R.-H.; Malaney, T. I.; Minasyan, R.; Pierschbacher, M. D.; Taulane, J. P.; Goodman, M. *Biopolymers* **2002**, *66*, 326–338.
18. (a) Kessler, H. *Angew. Chem., Int. Ed.* **1982**, *21*, 512–523. (b) Coles, M.; Sowemimo, V.; Scanlon, D.; Munro, S. L.; Craik, D. J. *J. Med. Chem.* **1993**, *36*, 2658–2665. (c) Mierke, D. F.; Kurz, M.; Kessler, H. *J. Am. Chem. Soc.* **1994**, *116*, 1042–1049. (d) Kessler, H.; Gemmecker, G.; Haupt, A.; Klein, M.; Wagner, K.; Will, M. *Tetrahedron* **1996**, *44*, 745–759. (e) Melacini, G.; Zhu, Q.; Ösapay, G.; Goodman, M. *J. Med. Chem.* **1997**, *40*, 2252–2258. (f) Mattern, R.-H.; Tran, T.-A.; Goodman, M. *J. Med. Chem.* **1998**, *41*, 2686–2692. (g) Yokokawa, F.; Sameshima, H.; In, Y.; Minoura, K.; Ishida, T.; Shioiri, T. *Tetrahedron* **2002**, *58*, 8127–8143.
19. ^{1}H NMR spectra of **1**–**6** were obtained in comparative experiments using the same conditions.
20. (a) Miyamoto, K.; Nakagawa, T.; Kuroda, Y. *J. Pept. Res.* **2001**, *58*, 193–203. (b) Miyamoto, K.; Nakagawa, T.; Kuroda, Y. *Biopolymers* **2001**, *59*, 380–393 and references cited therein.
21. In the recent review,[22] it was noticed that the ligand backbone conformations of **2** are similar between in the crystalline complex with $\alpha_v\beta_3$ integrin and in the ligand solution. In addition, a shorter distance between Arg and Asp C^α atoms of **1** was also observed in comparison with that of **2**.
22. Gottschalk, K.-E.; Kessler, H. *Angew. Chem., Int. Ed.* **2002**, *41*, 3767–3774.
23. Zhang, L.; Mattern, R.-H.; Malaney, T. I.; Pierschbacher, M. D.; Goodman, M. *J. Am. Chem. Soc.* **2002**, *124*, 2862–2863.
24. Pytela, R.; Pierschbacher, M. D.; Argraves, S.; Suzuki, S.; Rouslahti, E. *Methods Enzymol.* **1987**, *144*, 475–489.
25. Ludvigsen, S.; Andersen, K. V.; Poulsen, F. M. *J. Mol. Biol.* **1991**, *217*, 731–736.

Available online at www.sciencedirect.com
SCIENCE DIRECT®
Bioorganic & Medicinal Chemistry Letters
ELSEVIER
Bioorganic & Medicinal Chemistry Letters 16 (2006) 134–137

Design and synthesis of downsized metastin (45–54) analogs with maintenance of high GPR54 agonistic activity

Ayumu Niida,[a] Zixuan Wang,[b] Kenji Tomita,[a] Shinya Oishi,[a] Hirokazu Tamamura,[a] Akira Otaka,[a] Jean-Marc Navenot,[b] James R. Broach,[c] Stephen C. Peiper[b] and Nobutaka Fujii[a,*]

[a]*Graduate School of Pharmaceutical Sciences of Kyoto University, Sakyo-ku, Kyoto 606-8501, Japan*
[b]*Department of Pathology and Immunotherapy Center, Medical College of Georgia, Augusta, GA 30912, USA*
[c]*Department of Molecular Biology, Princeton University, Princeton, NJ 08544, USA*

Received 22 August 2005; revised 8 September 2005; accepted 12 September 2005
Available online 18 October 2005

Abstract—Metastin has been identified as a metastasis suppressor gene product that mediates its function through a G protein coupled receptor, GPR54. To refine insight into the critical pharmacophore for the activation of GPR54, we have conducted alanine and D-amino acid scanning on a biologically active metastin fragment (45–54). Based on these data and structures of peptides previously reported to activate GPR54, a series of shortened metastin (45–54) derivatives were synthesized and tested for the ability to induce GPR54 signaling. These biological experiments were performed in yeast containing human GPR54 that was coupled to the pheromone response pathway and a pheromone responsive *lacZ* reporter gene. Compounds **32**, **33**, and **39**, which possess an N-terminal basic group and a C-terminal RW-amide motif, were strong agonists, similar to the level of metastin. This may provide an approach to reverse the pro-metastatic effect of metastin deletion in multiple malignant tumors.

A metastasis suppressor gene that was originally designated KiSS1 was found to have decreased expression in metastatic melanoma, but not in non-metastatic counterparts.[1] The activity of this gene product was found to be mediated by an orphan GPCR (hOT7T175, AXOR12, GPR54).[2] Metastin, consisting of 54 amino acid residues, was recently identified as an endogenous ligand of GPR54 from a human placental extract.[2a] It was also demonstrated that this peptide was a post-translationally modified derivative of the 145 residues KiSS1/metastin precursor. The biological activity of metastin was localized to a 10 residues (45–54) C-terminally amidated peptide. Metastin (45–54) has been shown to oppose the proliferation and mobility of multiple tumor cell types in vitro. Clinical correlations in human tumors are limited to the finding of an inverse relationship between metastatic potential of malignant melanoma and KiSS1 expression by in situ hybridization.[3]

The biological significance of so-called 'Kisspeptins' is not limited to the negative regulation of the metastatic phenotype. KiSS1/metastin is expressed in placenta at high levels and lower copy numbers are detected in brain and testis.[2] The metastin receptor is expressed in placenta, brain, pituitary, spinal cord, pancreas, and carcinomas of the breast, ovary, and thyroid. Deficiency of metastin receptor function has been associated with hypogonadotropic hypogonadism in humans and genetically modified mouse models.[4]

Thus, metastin may be a candidate for a novel therapy to prevent metastatic spread of multiple malignancies, as well as having implications for hormonal therapy. The therapeutic use of metastin (45–54) possesses many limitations that include limited bioavailability and problematic stability. Downsizing and reduction of the peptide nature of metastin are critical to the future therapeutic targeting of its receptor in malignant and endocrine disorders. In this study we expressed the metastin receptor in yeast coupled to a pheromone-responsive *lacZ* reporter gene to select downsized metastin analogs possessing an N-terminal basic group and a C-terminal RW-amide motif.

Keywords: Metastin; GPR54 agonist.
* Corresponding author. Tel.: +81 75 753 4551; fax: +81 75 753 4570; e-mail: nfujii@pharm.kyoto-u.ac.jp

0960-894X/$ - see front matter © 2005 Elsevier Ltd. All rights reserved.
doi:10.1016/j.bmcl.2005.09.054

Ohtaki et al. described that N-terminally truncated metastin analog, metastin (45–54), possessed higher affinity for GPR54 compared to full length metastin, but metastin (46–54) was less potent.[2a] They presumed that C-terminally amidated sequence from Tyr^{45} to Phe^{54} is mostly involved in receptor interaction and that N-terminal portion of metastin is not essential for receptor binding, but it may be involved in another biological process such as stabilization and protection from proteolytic digestion. Therefore we envisioned that modification of metastin (45–54) would provide a novel low molecular GPR54 agonist.

First, we carried out Ala-scanning and D-amino acid scanning of metastin (45–54) in order to identify important residues for GPR54-agonistic activity. All peptides were synthesized by standard Fmoc-based solid phase peptide synthesis (Fmoc-SPPS). The activities of the peptides based on the structure of metastin (45–54) were determined in an assay system in yeast in which GPR54 was linked to the pheromone response signaling cascade via a hybrid G alpha subunit, modified from the approach previously described in our laboratory.[5] The agonistic activities of the synthetic peptides were determined by quantification of β-galactosidase activity encoded by a pheromone-sensitive *FUS1-lacZ* reporter gene. Following incubation with the candidate peptides for three hours at 37 °C, lysates were incubated with fluorescein di-β-D-galactopyranoside (FDG) (Molecular Probes, Eugene, OR), a fluorescent β-galactosidase substrate and analyzed in a FUSION (Packard) at appropriate excitation and emission wavelengths. The magnitude of GPR54 activation by the various mutants was compared to that of the metastin (45–54) parental template (Fig. 1).

In the Ala-scanning experiments, substitution of Phe^{50}, Leu^{52} and Phe^{54} resulted in complete loss of agonistic activities (peptides **6**, **8**, and **10**). The D-amino acid scanning showed the importance of stereochemistry of the C-terminal five residues for activation of GPR54 (peptides **16–20**). These data suggested that five amino acid residues, Phe^{50} to Phe^{54} play an especially important role for binding and activation of GPR54.

Recently, we reported that cyclic pentapeptide format can serve as an efficient template as a Pharmacophore displaying unit in the development of antagonists of the CXCR4 chemokine receptor.[6] It was reasoned that cyclic peptides containing Phe^{50} to Phe^{54} in metastin (45–54), which were shown to be important for the receptor activation in experiments described above, might show high agonistic activity because of the fixation of active conformation(s) by the ring structure.

We synthesized cyclic peptides **21–26** consisting of Ser^{46} to Phe^{54} without exchanging the order of the amino acids (Fig. 2). Gly^{51} was not deleted due to synthetic utility (racemization free, ease of cyclization). Protected peptides were constructed from Gly by Fmoc-SPPS on the 2-chlorotrityl resin. After cleavage from the resin without deprotection of side chain, the resulting peptides were cyclized by use of DPPA. Final deprotection with 95% TFA aq was followed by HPLC purification to yield the desired cyclic peptides. Agonistic activities of these peptides were evaluated by the pheromone-responsive *lacZ* reporter gene assay as described for the alanine scanning mutants. Disappointingly, these peptides showed no agonistic activities for GPR54 in this assay system.

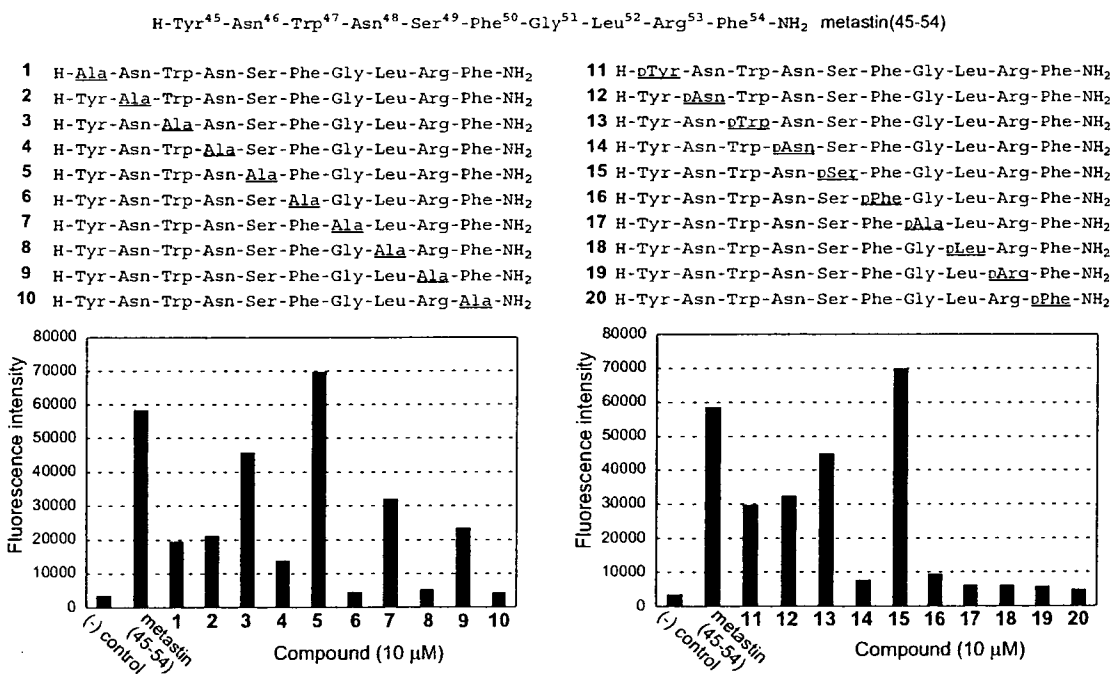

Figure 1. Ala-scanning and D-amino acid scanning of metastin (45–54) by *lacZ* reporter gene assay of GPR54-expressed in yeast.

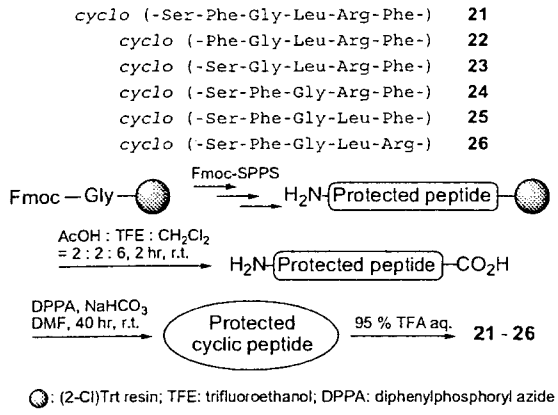

Figure 2. Synthetic scheme of cyclic peptides **21–26** and their sequences.

At the same time that metastin was identified as an endogenous ligand for GPR54, it was revealed that several invertebrate neuropeptides also possessed agonistic activity for this receptor. Some of sequences of reported peptides and their EC_{50} values determined by Clements et al. are shown in Table 1.[2b] It was confirmed that the potency of metastin and metastin (45–54) were more active than peptide **27** (reported EC_{50} (μM) value by Muir et al.[2c]: peptide 27: 1.86; metastin: 0.0012; metastin (45–54): 0.00050). The sequences of these peptides are similar to that of the metastin C-terminal region. Comparing peptide **28** with **29**, increased activity was associated with replacement of the C-terminal Phe with Trp. Peptide **30**, which contains an N-terminal side Arg as basic group and G-L-R-W-NH_2 sequence identical to the metastin C-terminus except for Trp residue, was the most potent of these short peptides. Therefore, modifications of metastin (45–54) were performed utilizing these data in order to develop downsized metastin analogs.

We designed several short metastin derivatives based on the sequence of metastin (45–54) (Fig. 3). All peptides possess an N-terminal basic group, for example a guanide group or a pyridine ring which are often found in GPCR ligands, and the C-terminal RW-amide motif. Several peptides were incorporated D-Phe-Pro, Phe-D-Ala or Phe-D-Pro sequence as a turn inducing spacer instead of Phe-Gly. All peptides were synthesized by standard Fmoc-SPPS. BisPy group and Gu group were constructed on the resin by reductive amination using 2-pyridinecarboxy aldehyde and $NaBH_3CN$ or commercially available guanilation reagent, respectively (Fig. 4).

The agonistic activities of these peptides were evaluated using the GPR54 pheromone responsive *lacZ* reporter gene in yeast (Fig. 5). In this experiment, peptides **32** (FM052a), **33** (FM053a), and **39** (FM059a) showed high agonistic activities at the same level as full length metastin. The molecular weights of these peptides (**32**: 992; **33**: 852; **39**: 1175) are lower than those of metastin and metastin (45–54) (5857 and 1302, respectively). Thus, the molecular size of metastin was dramatically downsized with maintenance of its agonistic potency. On the other hand, peptides **36–38** and **40–42**, which contained a turn inducing spacer, were less effective. The efficiencies of turn inducer for improvement of agonistic activity were not observed in this experiment.

In this study, Ala-scanning and D-amino acid scanning of metastin (45–54) were performed to determine the essential structures required for GPR54 agonistic activity. This analysis revealed that the C-terminal five residues of metastin (45–54) were critical to its GPR54 agonistic activity. Next, several metastin derivatives were synthesized based on the structures of metastin (45–54) and invertebrate neuropeptides previously reported as GPR54 agonists. It was demonstrated that significantly downsized analogs, including peptides **32**

Table 1. EC_{50} values of several invertebrate neuropeptides for human GPR54 reported by Clements et al.

Peptide	Sequence	EC_{50} (μM)
27	pEGLRW-NH_2	1.5
28	NRNFLRF-NH_2	8.0
29	NRNFLRW-NH_2	2.1
30	NRNGLRW-NH_2	0.2

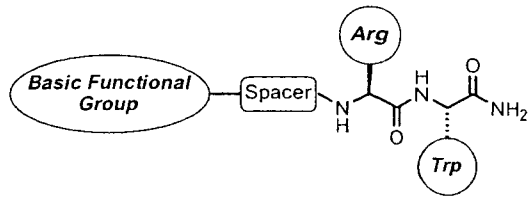

31	BisPy-desNLys-Phe-Gly-Leu-Arg-Trp-NH_2
32	BisPy-Amb-Phe-Gly-Leu-Arg-Trp-NH_2
33	Gu-Amb-Phe-Gly-Leu-Arg-Trp-NH_2
34	desNArg-Phe-Gly-Leu-Arg-Trp-NH_2
35	Ac-Arg-Phe-Gly-Leu-Arg-Trp-NH_2
36	Ac-Arg-DPhe-Pro-Leu-Arg-Trp-NH_2
37	Ac-Arg-Phe-DAla-Leu-Arg-Trp-NH_2
38	Ac-Arg-Phe-DPro-Leu-Arg-Trp-NH_2
39	Ac-Trp-Asn-Arg-Phe-Gly-Leu-Arg-Trp-NH_2
40	Ac-Trp-Asn-Arg-DPhe-Pro-Leu-Arg-Trp-NH_2
41	Ac-Trp-Asn-Arg-Phe-DAla-Leu-Arg-Trp-NH_2
42	Ac-Trp-Asn-Arg-Phe-DPro-Leu-Arg-Trp-NH_2

Figure 3. Sequences of short metastin derivatives. Abbreviations: BisPy: bis[(2-pyridinyl)methyl]; desNLys: 6-aminohexanoic acid; Amb: 4-aminomethylbenzoic acid; desNArg: 5-guanidinopentanoic acid; Gu: guanidino.

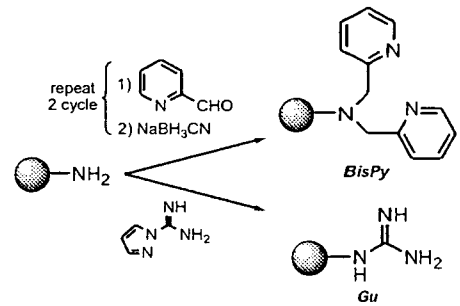

Figure 4. Constructions of BisPy group and Gu group on the resin.

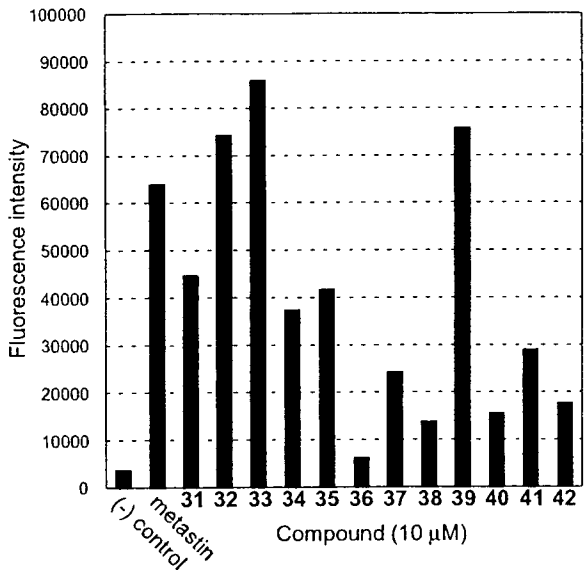

Figure 5. GPR54-agonistic activities of metastin and metastin shortened derivatives **31–42** in *lacZ* reporter gene assay on yeast.

(FM052a), **33** (FM053a) and **39** (FM059a), showed high agonistic activity, similar to the potency of metastin. These downsized peptides are potential lead compounds for development of a novel drug targeted to GPR54.

Acknowledgments

This research was supported in part by 21st Century COE Program 'Knowledge Information Infrastructure for Genome Science,' a Grant-in-Aid for Scientific Research from the Ministry of Education, Culture, Sports, Science and Technology, Japan Society for the Promotion of Science (JSPS), and the Japan Health Science Foundation. A.N. is grateful for Research Fellowships of the JSPS for Young Scientists.

Supplementary data

Supplementary data associated with this article can be found, in the online version, at doi:10.1016/j.bmcl.2005.09.054.

References and notes

1. Lee, J.-H.; Welch, D. R. *Int. J. Cancer* **1997**, *71*, 1035.
2. (a) Ohtaki, T.; Shintani, Y.; Honda, S.; Matsumoto, H.; Hori, A.; Kanehashi, K.; Terao, Y.; Kumano, S.; Takatsu, Y.; Masuda, Y.; Ishibashi, Y.; Watanabe, T.; Asada, M.; Yamada, T.; Suenaga, M.; Kitada, C.; Usuki, S.; Kurokawa, T.; Onda, H.; Nishimura, O.; Fujino, M. *Nature* **2001**, *411*, 613; (b) Clements, M. K.; McDonald, T. P.; Wang, R.; Xie, G.; O'Dowd, B. F.; George, S. R.; Austin, C. P.; Liu, Q. *Biochem. Biophys. Res. Commun.* **2001**, *284*, 1189; (c) Muir, A. I.; Chamberlain, L.; Elshourbagy, N. A.; Michalovich, D.; Moore, D. J.; Chalamari, A.; Szekeres, P. G.; Sarau, H. M.; Chambers, J. K.; Murdock, P.; Steplewski, K.; Shabon, U.; Miller, J. E.; Middleton, S. E.; Darker, J. G.; Larminie, C. G. C.; Wilson, S.; Bergsma, D. J.; Emson, P.; Faull, R.; Philpott, K. L.; Harrison, D. C. *J. Biol. Chem.* **2001**, *276*, 28969; (d) Horikoshi, Y.; Matsumoto, H.; Takatsu, Y.; Ohtaki, T.; Kitada, C.; Usuki, S.; Fujino, M. *J. Clin. Endocr. Metab.* **2003**, *88*, 914; (e) Hori, A.; Honda, S.; Asada, M.; Ohtaki, T.; Oda, K.; Watanabe, T.; Shintani, Y.; Yamada, T.; Suenaga, M.; Kitada, C.; Onda, H.; Kurokawa, T.; Nishimura, O.; Fujino, M. *Biochem. Biophys. Res. Commun.* **2001**, *286*, 958; (f) Kotani, M.; Detheux, M.; Vandenbogaerde, A.; Communi, D.; Vanderwinden, J.-M.; Le Poul, E.; Brézillon, S.; Tyldesley, R.; Suarez-Huerta, N.; Vandeput, F.; Blanpain, C.; Schiffmann, S. N.; Vassart, G.; Parmentier, M. *J. Biol. Chem.* **2001**, *276*, 34631; (g) Stafford, L. J.; Xia, C.; Ma, W.; Cai, Y.; Liu, M. *Cancer Res.* **2002**, *62*, 5399; (h) Terao, Y.; Kumano, S.; Takatsu, Y.; Hattori, M.; Nishimura, A.; Ohtaki, T.; Shintani, Y. *Biochim. Biophys. Acta.* **2004**, *1678*, 102.
3. (a) Shirasaki, F.; Takata, M.; Hatta, N.; Takehara, K. *Cancer Res.* **2001**, *61*, 7422; (b) Sanchez-Carbayo, M.; Capodieci, P.; Cordon-Cardo, C. *Am. J. Pathol.* **2003**, *162*, 609; (c) Ikeguchi, M.; Yamaguchi, K.; Kaibara, N. *Clin. Cancer Res.* **2004**, *10*, 1379; (d) Dhar, D. K.; Naora, H.; Kubota, H.; Maruyama, R.; Yoshimura, H.; Tonomoto, Y.; Tachibana, M.; Ono, T.; Otani, H.; Nagasue, N. *Int. J. Cancer* **2004**, *11*, 868.
4. (a) De Roux, N.; Genin, E.; Carel, J.-C.; Matsuda, F.; Chaussain, J.-L.; Milgrom, E. *Proc. Natl. Acad. Sci. U.S.A.* **2003**, *100*, 10972; (b) Seminara, S. B.; Messager, S.; Chatzidaki, E. E.; Thresher, R. R.; Acierno, J. S.; Shagoury, J. K.; Bo-Abbas, Y.; Kuohung, W.; Schwinof, K. M.; Hendrick, A. G.; Zahn, D.; Dixon, J.; Kaiser, U. B.; Slaugenhaupt, S. A.; Gusella, J. F.; O'Rahilly, S.; Carlton, M. B. L.; Crowley, W. F.; Aparicio, S. A. J. R.; Colledge, W. H. *N. Engl. J. Med.* **2003**, *349*, 1614; (c) Funes, S.; Hedrick, J. A.; Vassileva, G.; Markowitz, L.; Abbondanzo, S.; Golovko, A.; Yang, S.; Monsma, F. J.; Gustafson, E. L. *Biochem. Biophys. Res. Commun.* **2003**, *312*, 1357.
5. (a) Arias, D. A.; Navenot, J.-M.; Zhang, W.; Broach, J.; Peiper, S. C. *J. Biol. Chem.* **2003**, *278*, 36513; (b) Zhang, W.; Navenot, J.-M.; Haribabu, B.; Tamamura, H.; Hiramatsu, K.; Omagari, A.; Pei, G.; Manfredi, J. P.; Fujii, N.; Broach, J. R.; Peiper, S. C. *J. Biol. Chem.* **2002**, *277*, 24515.
6. Fujii, N.; Oishi, S.; Hiramatsu, K.; Araki, T.; Ueda, S.; Tamamura, H.; Otaka, A.; Kusano, S.; Terakubo, S.; Nakashima, H.; Broach, J. A.; Trent, J. O.; Wang, Z.; Peiper, S. C. *Angew. Chem., Int. Ed.* **2003**, *42*, 3251.

ARTICLE

OBC

www.rsc.org/obc

Structure–activity relationship studies on CXCR4 antagonists having cyclic pentapeptide scaffolds†

Hirokazu Tamamura,*[a,b] Ai Esaka,[b] Teppei Ogawa,[b] Takanobu Araki,[b] Satoshi Ueda,[b] Zixuan Wang,[c] John O. Trent,[d] Hiroshi Tsutsumi,[a] Hiroyuki Masuno,[a] Hideki Nakashima,[e] Naoki Yamamoto,[f] Stephen C. Peiper,[c] Akira Otaka[b,g] and Nobutaka Fujii*[b]

[a] *Institute of Biomaterials and Bioengineering, Tokyo Medical and Dental University, Chiyoda-ku, Tokyo, 101-0062, Japan. E-mail: tamamura.mr@tmd.ac.jp; Fax: +81 3 5280 8039; Tel: +81 3 5280 8036*

[b] *Graduate School of Pharmaceutical Sciences, Kyoto University, Sakyo-ku, Kyoto, 606-8501, Japan. E-mail: nfujii@pharm.kyoto-u.ac.jp; Fax: +81 75 753 4570; Tel: +81 75 753 4551*

[c] *Medical College of Georgia, Augusta, GA, 30912, USA*

[d] *James Graham Brown Cancer Center, University of Louisville, Louisville, KY, 40202, USA*

[e] *St. Marianna University, School of Medicine, Miyamae-ku, Kawasaki, 216-8511, Japan*

[f] *AIDS Research Center, National Institute of Infectious Diseases, Shinjuku-ku, Tokyo, 162-8640, Japan*

[g] *Graduate School of Pharmaceutical Sciences, The University of Tokushima, Tokushima, 770-8505, Japan*

Received 19th September 2005, Accepted 26th October 2005
First published as an Advance Article on the web 15th November 2005

Structure–activity relationship studies on CXCR4 antagonists, which were previously found by using cyclic pentapeptide libraries, were performed to optimize side-chain functional groups, involving conformationally constrained analogues. In addition, a new lead of cyclic pentapeptides with the introduction of a novel pharmacophore was developed.

Introduction

Chemokine receptors belong to a superfamily of seven transmembrane G-protein coupled receptors (7TM-GPCRs). An axis of a chemokine receptor, CXCR4, and its endogenous ligand, stromal cell-derived factor-1 (SDF-1/CXCL12),[1] has multiple important functions in normal physiology involving the migration of progenitors during embryologic development of the cardiovascular, hemopoietic and central nervous systems. This axis has been also recognized to be involved in several pathological conditions, such as HIV infection,[2] cancer metastasis/progression[3] and rheumatoid arthritis (RA).[4] Initially, CXCR4 was identified as a co-receptor that is used in the entry of T cell line-tropic (X4-) HIV-1 into T cells.[2] Subsequently, several papers reported that malignant cells from different types of cancer express CXCR4,[5] and that CXCL12 is highly expressed in the major metastatic destinations of the corresponding cancer,[3] suggesting that the interaction between CXCR4 and CXCL12 might determine the metastatic destination of cancer cells and cause organ preferential metastasis. Furthermore, Nanki *et al.* reported that CXCL12, which is highly expressed in the synovium of RA patients, stimulates migration of the memory T cells, which highly express CXCR4, thereby inhibits T cell apoptosis and leads to T cell accumulation in the RA synovium.[4a] Thus, CXCR4 is thought to be a great therapeutic target. A 14-mer peptide T140 and its analogues were previously found to be specific CXCR4 antagonists that were characterized as HIV-entry inhibitors,[6] anti-cancer-metastatic agents[3c] and anti-RA agents.[4b] The utilization of cyclic pentapeptide libraries involving the critical residues of T140, which were previously identified to be Arg^2, L-3-(2-naphthyl)alanine (Nal)[3], Tyr^5 and Arg^{14},[7] led to the finding of a cyclic pentapeptide FC131 [*cyclo*(-Arg^1-Arg^2-Nal^3-Gly^4-D-Tyr^5-)], which has strong CXCR4 antagonistic activity, comparable to that of T140 (Fig. 1).[8] Several FC131 analogues constrained or modified in Arg^1 were synthesized to find useful leads.[9] In this paper, we describe structure–activity relationship (SAR) studies on FC131 based on several synthetic analogues, which involve substitution for Arg^2, Nal^3 and D-Tyr^5. In addition, we attempt to incorporate a new pharmacophore such as a 4-fluorophenyl moiety, which was previously identified by the *N*-terminal modification of T140 analogs,[10] into cyclic pentapeptides.

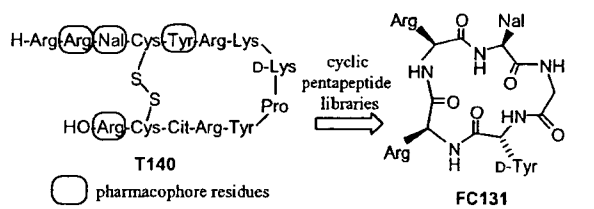

Fig. 1 Development of a low molecular weight CXCR4 antagonist FC131 based on cyclic pentapeptide libraries. Cit = L-citrulline.

Chemistry

Each peptide was synthesized in a general manner.[8] In the synthesis of compounds **6**, **7**, **9** and **10**, after cyclization and deprotection, *N*-guanylation of the resulting free side-chain amino group was performed with 1*H*-pyrazole-1-carboxamidine hydrochloride and DIPEA.[9]

Biological results and discussion

Several FC131 analogues, which have substitution for Arg^2, Nal^3 and D-Tyr^5, were prepared and assessed for CXCR4-binding activity based on inhibitory activity against CXCL12 binding to CXCR4.[11] First, analogues modified in the peripheral region of

† Electronic supplementary information (ESI) available: Characterization data (MS) of novel synthetic compounds. See DOI: 10.1039/b513145f

DOI: 10.1039/b513145f

Table 1 Inhibitory activity of cyclic pentapeptides involving substitution for Arg^2 in FC131 against CXCL12 binding to CXCR4

Compd	*cyclo*(-Arg^1-**X**-Nal^3-Gly^4-D-Tyr^5-) X	IC_{50}/μM[a]
1 (FC131)	Arg	0.0079
2	Ala	>1
3	Dab	0.44
4	Orn	0.69
5	Lys	>1
6	g-Dab	1.1
7	g-Lys	0.033
8	Glu	>1
9	*trans*-4-Guanidino-Pro	>1
10	*cis*-4-Guanidino-Pro	>1

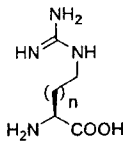

n = 1 γ-*N*-amidino-Dab (g-Dab)
n = 3 ε-*N*-amidino-Lys (g-Lys)

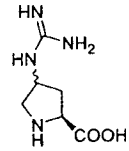

trans/*cis*-4-guanidino-Pro

[a] IC_{50} values are based on the inhibition of [^{125}I]-CXCL12 binding to CXCR4 transfectants of CHO cells. All data are mean values for at least three independent experiments.

Arg^2 were assayed (Table 1). Ala-substitution for Arg^2 in FC131 completely diminished the activity of the parent compound, whereas Ala-substitution for Arg^1 did not cause a severe decrease in potency,[9] suggesting that the side-chain of Arg^2 is very important for strong activity. Thus, optimization of the side-chain of Arg^2 was attempted by the synthesis of several analogues, where Arg^2 was replaced by Arg/Lys mimetics having various lengths of alkyl chains. L-2,4-Diaminobutyric acid (Dab)/L-ornithine (Orn)-substituted analogues, **3** and **4**, showed moderate CXCR4-binding activity, which is two orders of magnitude less potent than that of FC131, while a Lys-substituted analogue **5** did not show any significant activity until 1 μM. An ε-*N*-amidino-Lys (g-Lys)-substituted analogue, **7**, which has the side-chain with a one-carbon elongation compared to Arg^2, showed significant CXCR4-binding activity, which is 4-fold weaker than FC131. A γ-*N*-amidino-Dab (g-Dab)-substituted analogue, **6**, which has the side-chain with a one-carbon reduction compared to Arg^2, showed very low activity. It suggests that Arg is the most suitable at position 2 among the Arg/Lys mimetics used in this study. A Glu-substituted analogue, **8**, did not show any significant activity until 1 μM, suggesting that a basic functional group, such as an amino or guanidino group, in the side-chain of the amino acid at position 2 is indispensable for binding to CXCR4. In our previous study, analogues, in which a conformationally constrained Arg mimetic, *trans*- or *cis*-4-guanidino-Pro, was incorporated at position 1, showed higher CXCR4-binding activity than a g-Dab-substituted analogue, having the same length of the linear-type side chain of the amino acid at position 1.[9] Thus, in this study, analogues, in which *trans*- or *cis*-4-guanidino-Pro was incorporated at position 2, were prepared and assessed for CXCR4-binding activity. However, the conformationally constrained analogues, **9** and **10**, did not show any significant activity until 1 μM. This proved that fixing the backbone and the side-chain of Arg^2 is not suitable.

Second, analogues modified in the peripheral region of Nal^3 were assayed (Table 2). Ala-substitution for Nal^3 in FC131 completely diminished the activity of the parent compound. Since the side-chain of Nal^3 is indispensable for strong activity, optimization of the side-chain of Nal^3 was attempted by the synthesis of several analogues, where Nal^3 was replaced by Trp mimetics. A Trp-substituted analogue, **12**, showed strong CXCR4-binding activity, which is slightly less potent than

Table 2 Inhibitory activity of cyclic pentapeptides involving substitution for Nal^3 in FC131 against CXCL12 binding to CXCR4

Compd	*cyclo*(-Arg^1-Arg^2-**X**-Gly^4-D-Tyr^5-) X	IC_{50}/μM
1 (FC131)	Nal	0.0079
11	Ala	>1
12	Trp	0.013
13	Tpi	>1
14	Bth	0.018
15	D-Bth	0.26

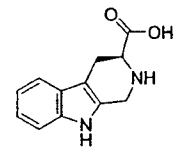

(3*S*)-2,3,4,9-tetrahydro-1*H*-β-carboline-3-carboxylic acid (Tpi)

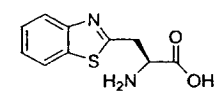

(2*S*)-2-amino-3-benzothiazol-2-yl-propionic acid (Bth)

that of FC131. This is compatible with our previous result: T140 is more potent than T134 [Trp^3-T140].[6] A (3*S*)-2,3,4,9-tetrahydro-1*H*-β-carboline-3-carboxylic acid (Tpi)-substituted analogue, **13**, which is conformationally constrained in the backbone and the side-chain of the amino acid at position 3, did not show any significant activity until 1 μM, suggesting that fixing the backbone and the side-chain of Trp (or Nal^3) is not suitable. A (2*S*)-2-amino-3-benzothiazol-2-yl-propionic acid (Bth)-substituted analogue, **14**, showed strong CXCR4-binding activity, which is almost the same as that of the Trp-substituted analogue, **12**. D-Bth-substituted analogue, **15**, is 14-fold less potent than **14**. This is also compatible with our previous result: D-Nal^3-FC131 is 20-fold less potent than FC131.[8] Taken together, Nal is more suitable at position 3 than any other Trp-mimetics.

Third, analogues modified in the peripheral region of D-Tyr^5 were assayed (Table 3). D-Ala-substitution for D-Tyr^5 in FC131 also diminished the activity of the parent compound. Optimization of the side-chain of D-Tyr^5 was attempted by the synthesis of several analogues, where D-Tyr^5 was replaced by D-Tyr/Phe mimetics. A D-Phe(4-NH_2)-substituted analogue, **17**, and a D-Phe(4-OMe)-substituted analogue, **18**, which have electron-donating substituents on the aromatic ring of the amino acid at position 5, showed remarkably less potent CXCR4-binding activity than FC131, which also has an electron-donating substituent on the aromatic ring. The analogues, **17** and **18**, were weaker than a D-Phe-substituted analogue,

Table 3 Inhibitory activity of cyclic pentapeptides involving substitution for D-Tyr^5 in FC131 against CXCL12 binding to CXCR4

Compd	*cyclo*(-Arg^1-Arg^2-Nal^3-Gly^4-**X**^{5}-) X	IC_{50}/μM
1 (FC131)	D-Tyr	0.0079
16	D-Ala	>1
17	4-Amino-D-phenylalanine [D-Phe(4-NH_2)]	0.10
18	4-Methoxy-D-phenylalanine [D-Phe(4-OMe)]	0.51
19	D-His	0.15
20	D-Phe	0.051
21	4-Fluoro-D-phenylalanine [D-Phe(4-F)]	0.22
22	D-Tic(7-OH)	0.16

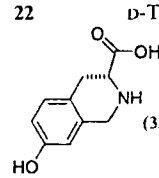

(3*R*)-7-Hydroxy-1,2,3,4-tetrahydro-isoquinoline-3-carboxylic acid [D-Tic(7-OH)]

Table 4 Inhibitory activity of cyclic pentapeptides involving the incorporation of Phe(4-F)^1 into FC131 against CXCL12 binding to CXCR4

Compd	Sequence	IC_{50}/μM
1 (FC131)	*cyclo*(-Arg^1-Arg^2-Nal^3-Gly^4-D-Tyr^5-)	0.0079
23	*cyclo*(-Phe(4-F)^1-Arg^2-Nal^3-Gly^4-D-Tyr^5-)	0.057
24	*cyclo*(-Phe(4-F)^1-Arg^2-Nal^3-Gly^4-Arg^5-)	0.62
25	*cyclo*(-D-Phe(4-F)^1-Arg^2-Nal^3-Gly^4-Arg^5-)	0.035
26	*cyclo*(-Phe(4-F)^1-Arg^2-Nal^3-Gly^4-D-Arg^5-)	0.088
27	*cyclo*(-D-Phe(4-F)^1-Arg^2-Nal^3-Gly^4-D-Arg^5-)	0.094
28	*cyclo*(-D-Tyr^1-Arg^2-Nal^3-Gly^4-Arg^5-)	0.30

20. Thus, an electron-donating substituent on the aromatic ring of the amino acid at position 5 is not always suitable for strong CXCR4-binding activity. On the other hand, a D-Phe(4-F)-substituted analogue, **21**, which has an electron-withdrawing substituent on the aromatic ring, was also less potent than FC131 or the D-Phe-substituted analogue, **20**. A D-His-substituted analogue, **19**, which has a basic/aromatic amino acid at position 5, did not show stronger activity than **20**. A (3*R*)-7-hydroxy-1,2,3,4-tetrahydro-isoquinoline-3-carboxylic acid [D-Tic(7-OH)]-substituted analogue, **22**, which is conformationally constrained in the backbone and the side-chain of the amino acid at position 5, showed remarkably less potent CXCR4-binding activity than FC131, suggesting that fixing the backbone and the side-chain of D-Tyr^5 is also not suitable. Taken together, D-Tyr is the most suitable at position 5 among the tested amino acids without any relation to the electron-withdrawing or -donating effect of the substituent on the aromatic ring.

Recently, a novel pharmacophore of T140-related CXCR4 antagonists, such as a 4-fluorophenyl moiety, was found in addition to the original pharmacophores of T140, Arg (x 2), Nal and Tyr.[10] Fourth, since the phenol group of D-Tyr^5 could not be replaced by the 4-fluorophenyl group with maintenance of high activity, as seen in the D-Phe(4-F)-substituted analogue, **21**, we attempted to incorporate the 4-fluorophenyl group into the amino acid at position 1. [Phe(4-F)^1]-FC131, **23**, showed significant CXCR4-binding activity, which is less potent than that of FC131. Since another Arg residue is thought to be indispensable for high activity and an aromatic residue [L/D-Phe(4-F)] is incorporated into position 1, we tried to replace D-Tyr^5 by L/D-Arg^5. Four analogues, **24–27**, [L/D-Phe(4-F)^1, L/D-Arg^5]-FC131, were prepared and assayed (Table 4). Among these compounds [D-Phe(4-F)^1, Arg^5]-FC131, **25**, showed the most potent activity, which is 10-fold more potent than that of [D-Tyr^1, Arg^5]-FC131, **28**. Thus, it is thought that [D-Phe(4-F)^1, Arg^5]-FC131, **25**, is useful as a novel lead involving the pharmacophores different from FC131, although **25** is 4-fold less potent than FC131.

Conclusion

In summary, SAR studies on cyclic pentapeptides having CXCR4-antagonistic activity, such as FC131, were performed. Several analogues were synthesized to optimize side-chain functional groups, involving constrained analogues that conformationally fix the backbone and the side-chains. Taken together, Arg, Nal and D-Tyr are the most suitable at position 2, 3 and 5, respectively, than any other corresponding amino acid mimetics that were tested in the present study. Furthermore, a novel lead compound, which contains a 4-fluorophenyl group as the new pharmacophore, was found.

Acknowledgements

This work was supported in part by a 21st Century COE Program "Knowledge Information Infrastructure for Genome Science", a Grant-in-Aid for Scientific Research from the Ministry of Education, Culture, Sports, Science and Technology, Japan, the Japan Health Science Foundation and Philip Morris USA Inc. and Philip Morris International. S. U. is grateful for a Research Fellowship from the Japan Society for the Promotion of Science for Young Scientists.

References

1 (*a*) T. Nagasawa, H. Kikutani and T. Kishimoto, *Proc. Natl. Acad. Sci. U. S. A.*, 1994, **91**, 2305; (*b*) C. C. Bleul, M. Farzan, H. Choe, C. Parolin, I. Clark-Lewis, J. Sodroski and T. A. Springer, *Nature*, 1996, **382**, 829; (*c*) E. Oberlin, A. Amara, F. Bachelerie, C. Bessia, J.-L. Virelizier, F. Arenzana-Seisdedos, O. Schwartz, J.-M. Heard, I. Clark-Lewis, D. F. Legler, M. Loetscher, M. Baggiolini and B. Moser, *Nature*, 1996, **382**, 833; (*d*) K. Tashiro, H. Tada, R. Heilker, M. Shirozu, T. Nakano and T. Honjo, *Science*, 1993, **261**, 600.

2 Y. Feng, C. C. Broder, P. E. Kennedy and E. A. Berger, *Science*, 1996, **272**, 872.

3 (*a*) T. Koshiba, R. Hosotani, Y. Miyamoto, J. Ida, S. Tsuji, S. Nakajima, M. Kawaguchi, H. Kobayashi, R. Doi, T. Hori, N. Fujii and M. Imamura, *Clin. Cancer Res.*, 2000, **6**, 3530; (*b*) A. Müller, B. Homey, H. Soto, N. Ge, D. Catron, M. E. Buchanan, T. McClanahan, E. Murphy, W. Yuan, S. N. Wagner, J. L. Barrera, A. Mohar, E. Verastegui and A. Zlotnik, *Nature*, 2001, **410**, 50; (*c*) H. Tamamura, A. Hori, N. Kanzaki, K. Hiramatsu, M. Mizumoto, H. Nakashima, N. Yamamoto, A. Otaka and N. Fujii, *FEBS Lett.*, 2003, **550**, 79; (*d*) N. Tsukada, J. A. Burger, N. J. Zvaifler and T. J. Kipps, *Blood*, 2002, **99**, 1030; (*e*) J. Juarez, K. F. Bradstock, D. J. Gottlieb and L. J. Bendall, *Leukemia*, 2003, **17**, 1294.

4 (*a*) T. Nanki, K. Hayashida, H. S. El-Gabalawy, S. Suson, K. Shi, H. J. Girschick, S. Yavuz and P. E. Lipsky, *J. Immunol.*, 2000, **165**, 6590; (*b*) H. Tamamura, M. Fujisawa, K. Hiramatsu, M. Mizumoto, H. Nakashima, N. Yamamoto, A. Otaka and N. Fujii, *FEBS Lett.*, 2004, **569**, 99.

5 F. Balkwill, *Semin. Cancer Biol.*, 2004, **14**, 171.

6 H. Tamamura, Y. Xu, T. Hattori, X. Zhang, R. Arakaki, K. Kanbara, A. Omagari, A. Otaka, T. Ibuka, N. Yamamoto, H. Nakashima and N. Fujii, *Biochem. Biophys. Res. Commun.*, 1998, **253**, 877.

7 H. Tamamura, A. Omagari, S. Oishi, T. Kanamoto, N. Yamamoto, S. C. Peiper, H. Nakashima, A. Otaka and N. Fujii, *Bioorg. Med. Chem. Lett.*, 2000, **10**, 2633.

8 N. Fujii, S. Oishi, K. Hiramatsu, T. Araki, S. Ueda, H. Tamamura, A. Otaka, S. Kusano, S. Terakubo, H. Nakashima, J. A. Broach, J. O. Trent, Z. Wang and S. C. Peiper, *Angew. Chem., Int. Ed.*, 2003, **42**, 3251.

9 H. Tamamura, T. Araki, S. Ueda, Z. Wang, S. Oishi, A. Esaka, J. O. Trent, H. Nakashima, N. Yamamoto, S. C. Peiper, A. Otaka and N. Fujii, *J. Med. Chem.*, 2005, **48**, 3280.

10 H. Tamamura, K. Hiramatsu, M. Mizumoto, S. Ueda, S. Kusano, S. Terakubo, M. Akamatsu, N. Yamamoto, J. O. Trent, Z. Wang, S. C. Peiper, H. Nakashima, A. Otaka and N. Fujii, *Org. Biomol. Chem.*, 2003, **1**, 3663.

11 H. Tamamura, K. Hiramatsu, S. Ueda, Z. Wang, S. Kusano, S. Terakubo, J. O. Trent, S. C. Peiper, N. Yamamoto, H. Nakashima, A. Otaka and N. Fujii, *J. Med. Chem.*, 2005, **48**, 380.

Expert Opinion

Ashley Publications
www.ashley-pub.com

General

The therapeutic potential of CXCR4 antagonists in the treatment of HIV infection, cancer metastasis and rheumatoid arthritis

Hirokazu Tamamura & Nobutaka Fujii†
†*Graduate School of Pharmaceutical Sciences, Kyoto University, Sakyo-ku, Kyoto 606-8501, Japan*

CXCR4 is the receptor of the chemokine CXCL12, which is involved in progression and metastasis of several types of cancer cells, HIV infection and rheumatoid arthritis. The authors developed selective CXCR4 antagonists, T22 and T140, initially as anti-HIV agents, which inhibit T cell line-tropic (X4-) HIV-1 infection through their specific binding to CXCR4. Recently, T140 analogues have also been shown to inhibit CXCL12-induced migration of breast cancer cells, leukaemia T cells, pancreatic cancer cells, small cell lung cancer cells, chronic lymphocytic leukaemia B cells, pre-B acute lymphoblastic leukaemia cells and so on *in vitro*. Biostable T140 analogues significantly suppressed pulmonary metastasis of breast cancer cells and melanoma cells in mice. Furthermore, these compounds significantly suppressed the delayed-type hypersensitivity response induced by sheep red blood cells and collagen-induced arthritis, which represent *in vivo* mouse models of arthritis. Thus, T140 analogues proved to be attractive lead compounds for chemotherapy of these problematic diseases. This article reviews recent research on T140 analogues, referring to several other CXCR4 antagonists.

Keywords: cancer cell progression, cancer metastasis, chemokine receptor, HIV infection, low molecular weight CXCR4 antagonist, rheumatoid arthritis (RA), T140, T22

Expert Opin. Ther. Targets (2005) 9(6):1267-1282

1. Introduction

The chemokine receptor CXCR4 is a seven transmembrane G-protein-coupled receptor (GPCR), which transduces signals of the chemokine, CXCL12/stromal cell-derived factor-1 (SDF-1) [1-4]. The CXCL12–CXCR4 axis plays an important role in the migration of progenitors during embryonic development of the cardiovascular, haemopoietic, central nervous systems etc. This system has also been shown to be involved in several problematic diseases, including HIV infection [5], cancer cell metastasis/progression [6-26] and rheumatoid arthritis (RA) [27] (**Figure 1**). CXCR4 was initially identified as a co-receptor that is utilised by T cell line-tropic (X4-) HIV-1 strains [5]. X4 HIV-1 strains constitute the majority in the late stage of HIV infection and AIDS, whereas macrophage-tropic (R5-) HIV-1 strains, which use the chemokine receptor CCR5 as another co-receptor, do in the early stage of HIV infection [28-32]. Müller *et al.* revealed that CXCR4 and another chemokine receptor, CCR7, are highly expressed in the surface of human breast cancer cells, whereas CXCL12 and a CCR7 ligand, CCL21, are highly expressed in lymph nodes, bone marrow, lung and liver, which constitute the common metastatic destinations of breast cancer, suggesting that the CXCL12–CXCR4 axis might determine the metastatic destination of

10.1517/14728222.9.6.1267 ISSN 1472-8222

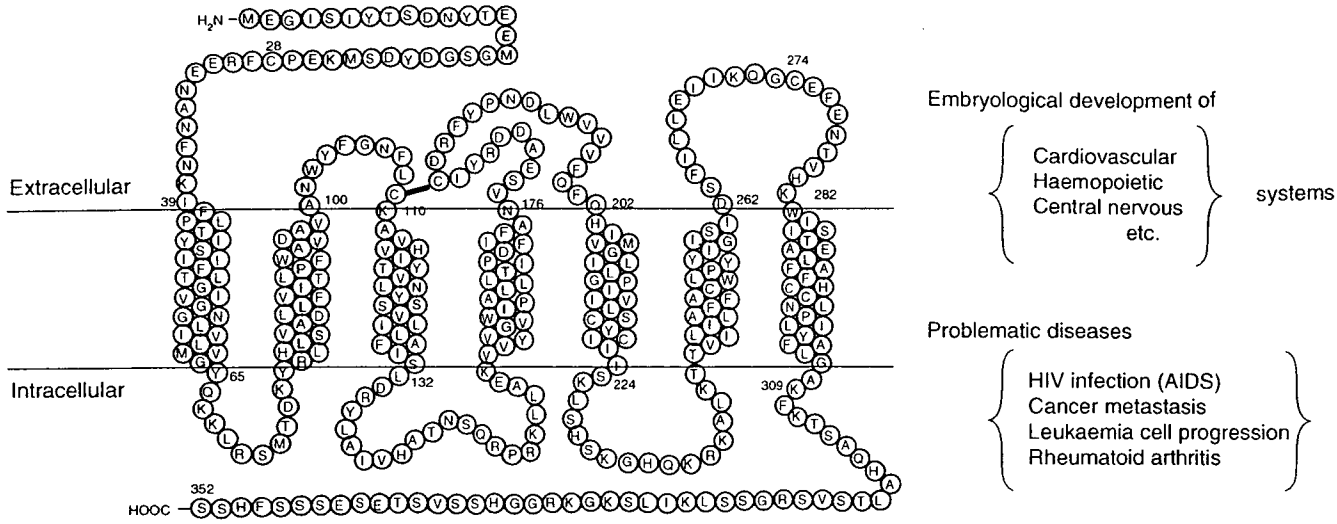

Figure 1. CXCR4 [5] and its actions.

tumour cells and cause organ preferential metastasis [6]. CXCR4 is expressed on malignant cells from at least 23 different types of cancer [33], including pancreatic cancer cells [7,8], melanoma cells [6,9,10], prostate cancer cells [11], kidney cancer cells [12], neuroblastoma cells [13], non-Hodgkin's lymphoma cells [14], small cell lung cancer (SCLC) cells [15,16], ovarian cancer cells [17,18], multiple myeloma cells [19,20], chronic lymphocytic leukaemia (CLL) B cells [21,22], pre-B acute lymphoblastic leukaemia (ALL) cells [23] and malignant brain tumour cells [24]. RA is an annoying disorder, which is mainly caused by the $CD4^+$ memory T cell accumulation in the inflamed synovium. Nanki *et al.* reported that the memory T cells highly express CXCR4 and the CXCL12 concentration is extremely high in the synovium of RA patients, and that CXCL12 stimulates migration of the memory T cells and inhibits T cell apoptosis, indicating that the CXCL12–CXCR4 interaction plays a critical role in T cell accumulation in the RA synovium [27]. Thus, CXCR4 is thought to be an important therapeutic target for the above diseases. This review article focuses on the development of CXCR4 antagonists, including several antagonists reported by other groups.

2. Discovery of T22 and T140 as selective inhibitors for the HIV co-receptor CXCR4

To date, the molecular mechanism concerning HIV-1 replication has been elucidated in detail, especially for a dynamic supramolecular mechanism relevant to HIV entry/fusion steps: Initially, an HIV envelope protein gp120 interacts with a cell surface protein CD4, which leads to a conformational change of gp120 followed by its subsequent binding to the second cellular receptor, CCR5 [28–32] or CXCR4 [5]. Next, the interaction of gp120 with CCR5 or CXCR4 causes penetration of an envelope subunit, gp41, which anchors the HIV envelope into membrane, to the cell membrane from the *N*-terminus end and subsequent formation of the gp41 trimer-of-hairpins structure in the centre region, which leads to membrane fusion of HIV/cells and thereby results in completion of the infection [34]. Elucidation of the above dynamic molecular machinery prompted many researchers to develop effective inhibitors blocking HIV-entry/fusion steps targeting the second receptors, CCR5 and CXCR4, and the dynamic process involving formation of the gp41 trimer-of-hairpins structure.

Highly active antiretroviral therapy (HAART), which uses a combination of two (or more) different agents that are usually adopted from two drug categories (reverse transcriptase inhibitors and protease inhibitors), has brought a significant, but partial, success and hope in the clinical treatment of AIDS or HIV-1-infected patients, whereas there still remain several serious problems even with HAART, which involve the emergence of viral strains with multi-drug resistance (MDR), considerable adverse effects and high costs [35,36]. An ideal therapeutic approach would block the HIV entry/fusion steps, as described above. Thus, the authors' research has focused on drug discovery targeting co-receptors and gp41. A review referring to CCR5 antagonists and gp41-targeting fusion inhibitors is reported elsewhere [37].

Tachyplesins and polyphemusins show antibacterial and antiviral activity as 17-mer and 18-mer self-defence peptides that were isolated from the haemocyte debris of the Japanese horseshoe crab (*Tachypleus tridentatus*) and the American horseshoe crab (*Limulus polyphemus*), respectively [38,39]. The authors' previous structure–activity relationship (SAR) study on these peptides led to development of an anti-HIV peptide, T22 ([Tyr5, 12, Lys7]-polyphemusin II) [40,41] and its shortened 14-mer peptide, T140 (**Figure 2**) [42]. T22 and T140 proved to strongly block an X4-HIV-1 entry through their specific binding to CXCR4 and to inhibit Ca^{2+} mobilisation induced by CXCL12 stimulation through CXCR4 [43-45].